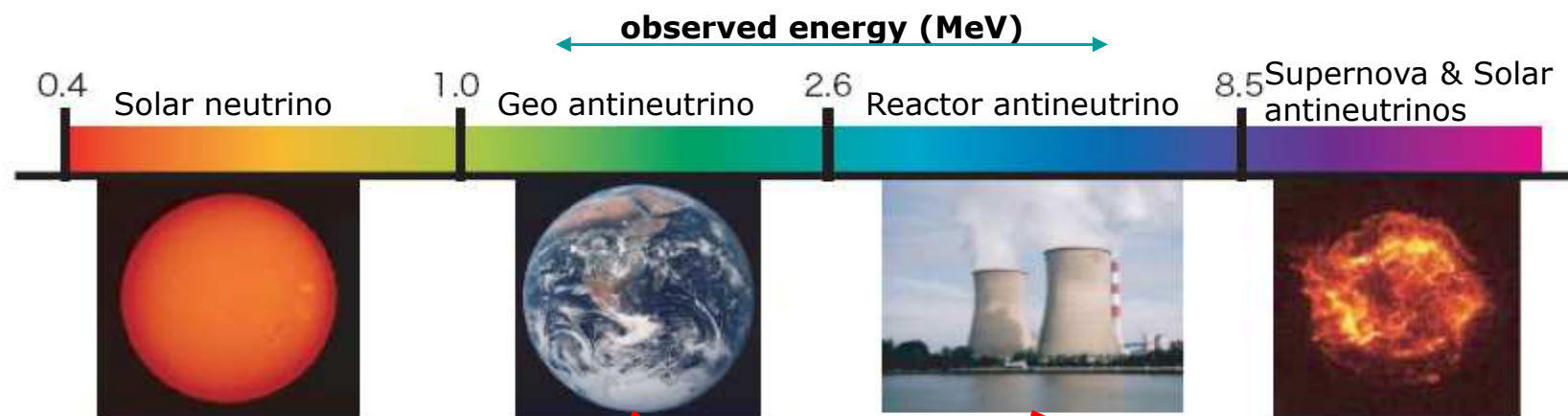


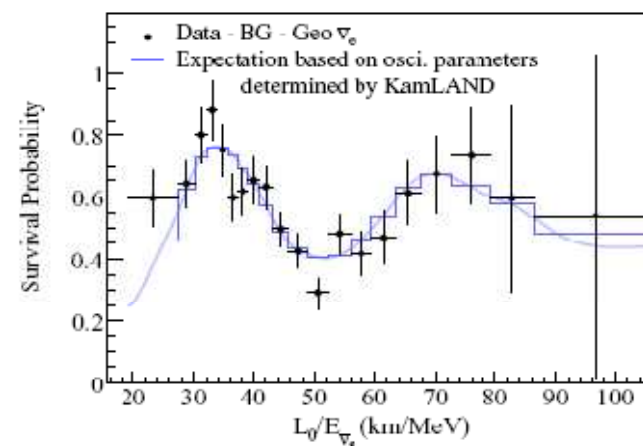
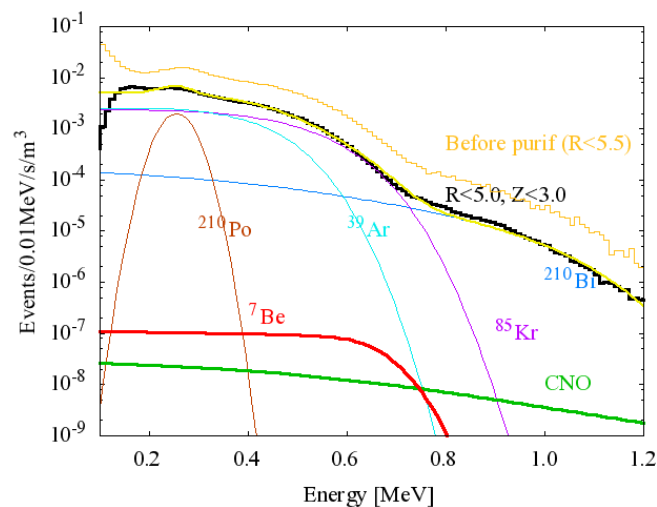
# Search for electron anti-neutrinos from the Sun with KamLAND detector

Oleg Perevozchikov, University of Tennessee  
HEP Seminar at University of Virginia  
October 7, 2009

# Physics in KamLAND



work in progress

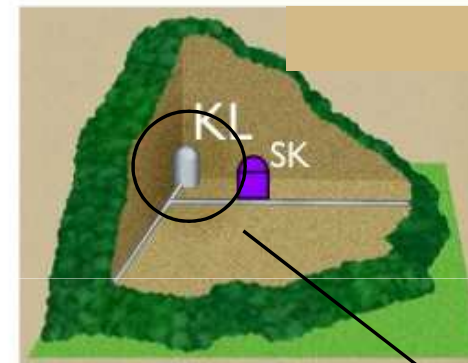


# Kamioka Liquid-scintillator Anti-neutrino Detector (KamLAND)



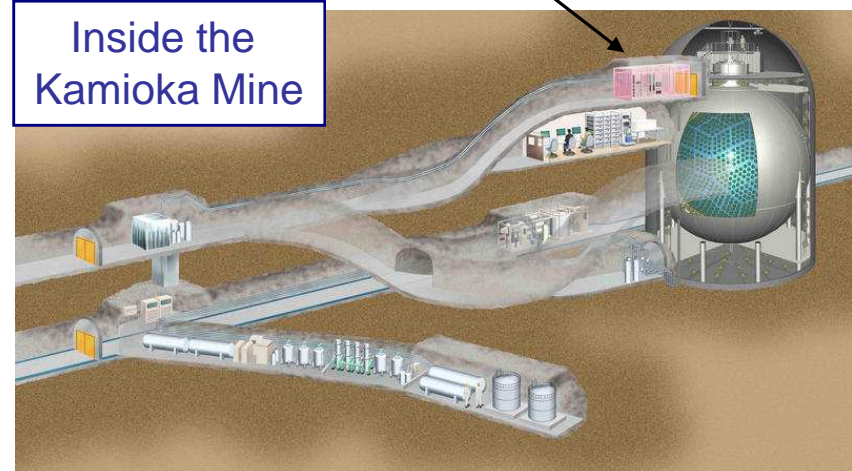
Surrounded by 55 Japanese Reactor Units

Detecting reactor  $\bar{\nu}_e$  1km beneath Mt. Ikenoyama

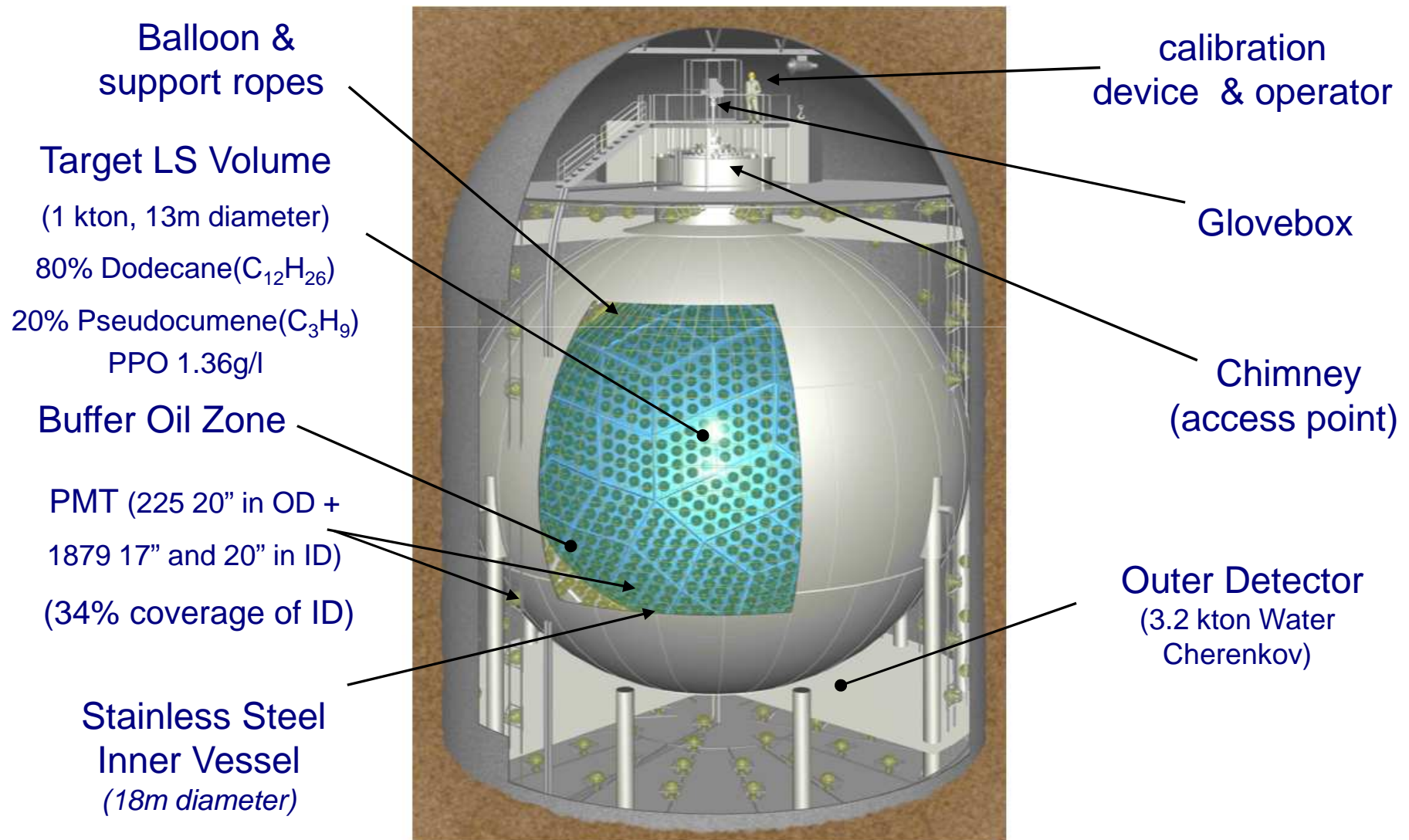


1000m rock  
= 2700 mwe

Inside the  
Kamioka Mine



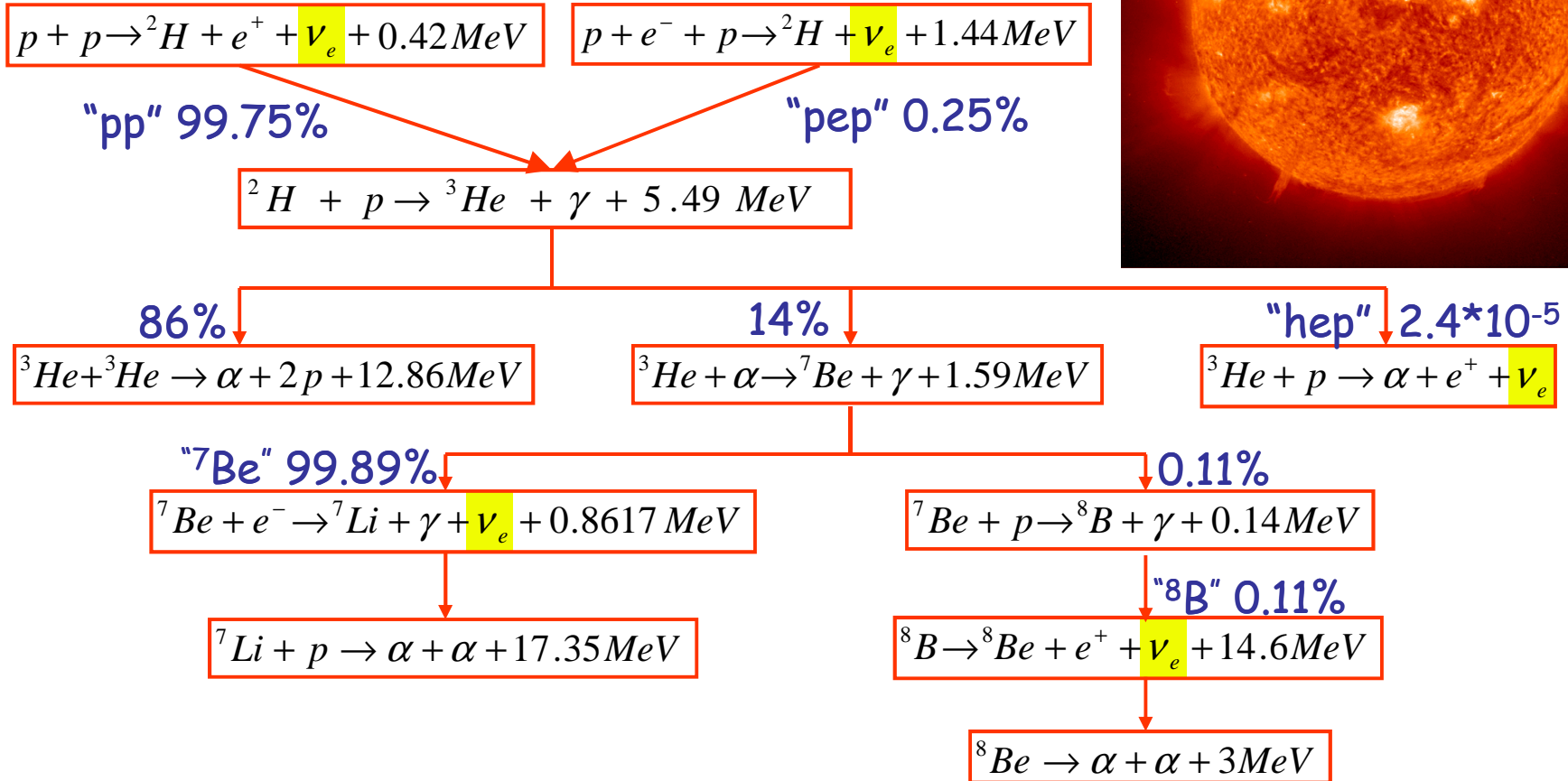
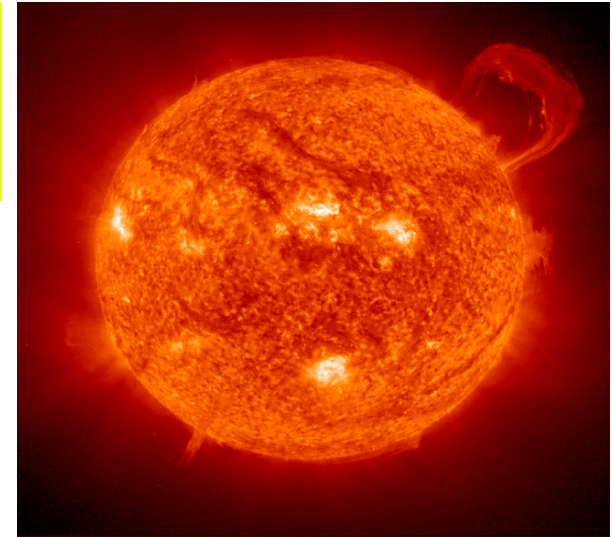
# The KamLAND Detector





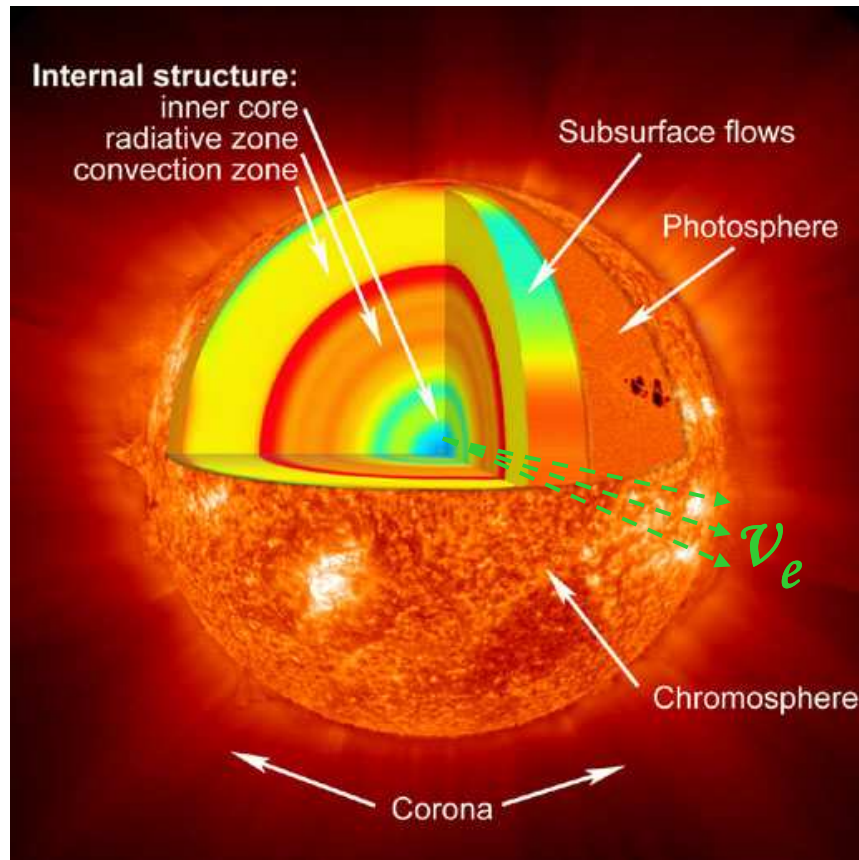
# Solar Neutrinos Production (pp-chain)

$\nu_e$  are abundant by-products of nuclear fusion in the sun



No direct production of  $\bar{\nu}_e$

# Conversion Mechanism of Neutrinos

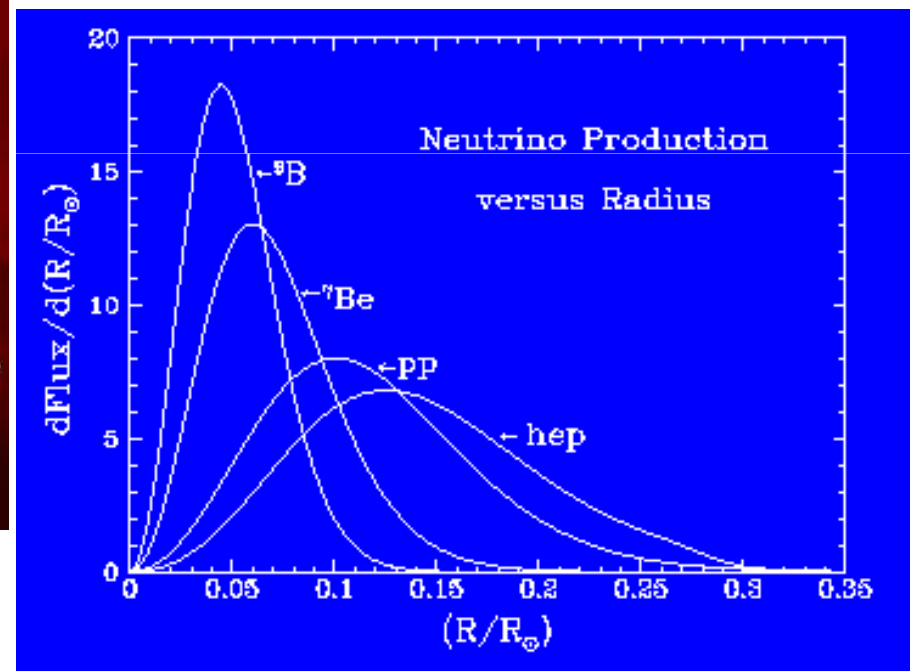


**Sun Layers**

E. Akhmedov and J Pulido, Phys. Lett B 553, 7 (2003)

$$\nu_{eL} \xrightarrow{\text{SFP}} \bar{\nu}_{\mu R} \xrightarrow{\text{osc.}} \bar{\nu}_{eR}$$

$B_T \sim 10^7 \text{G}$       Vacuum oscillations



**$\nu_e$  production as function of radius**

# SFP and Oscillations

Neutrino flavor eigenstates:  $\nu_e, \nu_\mu, \nu_\tau$  Neutrino mass eigenstates:  $\nu_1, \nu_2, \nu_3$

General form of connection between mass and flavor eigenstates

$$|\nu_\alpha\rangle = \sum_{j=1}^3 U_{\alpha j} |\nu_j\rangle, \quad \alpha = e, \mu, \tau$$

$$U = \begin{pmatrix} 1 & 0 & 0 \\ 0 & c_{23} & s_{23} \\ 0 & -s_{23} & c_{23} \end{pmatrix} \begin{pmatrix} c_{23} & 0 & s_{13}e^{-i\delta} \\ 0 & 1 & 0 \\ -s_{13}e^{i\delta} & 0 & c_{13} \end{pmatrix} \begin{pmatrix} c_{12} & s_{12} & 0 \\ -s_{12} & c_{12} & 0 \\ 0 & 0 & 1 \end{pmatrix},$$

$$s_{ij} = \sin \theta_{ij}, c_{ij} = \cos \theta_{ij} (i, j = 1, 2, 3)$$

**Time evolution of the states:**

$$i \frac{d}{dt} |\nu_j\rangle = E_j |\nu_j\rangle \Rightarrow |\nu_j(t)\rangle = e^{-iE_j t} |\nu_j(0)\rangle$$

$$|\nu_\alpha(t)\rangle = \sum_{j=1}^3 U_{\alpha j} e^{-iE_j t} U_{j\alpha}^\dagger |\nu_\alpha(0)\rangle$$

**Oscillation probability for the simple case (only 2 flavor):**

$$P(\nu_\alpha \rightarrow \nu_\beta) = \sin^2 2\theta_\nu \sin^2 \left( \frac{1.27 \Delta m^2 [eV^2] L [m]}{E [MeV]} \right)$$

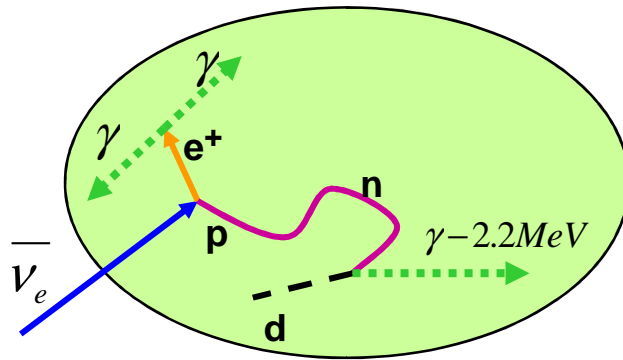
**SFP at magnetic field & non zero neutrino magnetic moment**

$$P(\nu_{eL} \rightarrow \bar{\nu}_{\mu R}) = 3.6 \times 10^{-10} \left[ \frac{\mu}{10^{-12} \mu_B} \frac{B_T(0.05 R_{sun})}{10 kG} \right]^2 \quad (\text{E. Akhmedov and J Pulido, Phys. Lett B 553, 7 (2003)})$$

**Final conversion probability:**

$$P(\nu_{eL} \rightarrow \bar{\nu}_{eR}) = 1.8 \times 10^{-10} \left[ \frac{\mu_\nu}{10^{-12} \mu_B} \times \frac{B_T(0.05 R_s)}{10 kG} \right]^2 \sin^2 2\theta_{12}$$

# Antineutrino detection



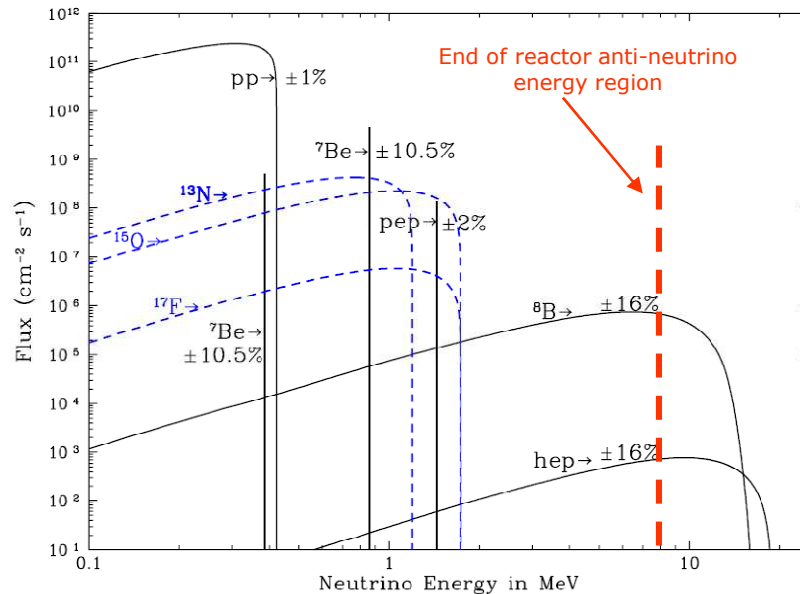
Prompt - Inverse  $\beta$ -decay:

$$\bar{\nu}_e + p \rightarrow e^+ + n, E_{\text{threshold}} = 1.8 \text{ MeV}$$

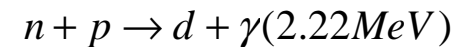
$$\sigma_{\bar{\nu}_e + p \rightarrow e^+ + n} [\text{cm}^2] = 9.3 \times 10^{-44} \left( \frac{E_{\bar{\nu}}}{1 \text{ MeV}} \right)^2 \left( 1 - \frac{Q}{E_{\bar{\nu}}} \right) \sqrt{1 - 2 \frac{Q}{E_{\bar{\nu}}} + \frac{Q^2 - m_e^2}{E_{\bar{\nu}}^2}} \Theta(E_{\bar{\nu}})$$

$$Q = M_n - M_p, \Theta(E_{\bar{\nu}}) = \begin{cases} 1, & E_{\bar{\nu}} > Q \\ 0, & E_{\bar{\nu}} < Q \end{cases}$$

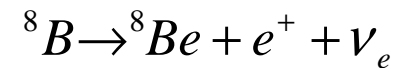
## Solar neutrino spectrum



Delayed - Neutron capture ( $\sim 220 \mu\text{sec}$ ):



KamLAND can be sensitive only to conversion of  $^8\text{B}$  neutrinos

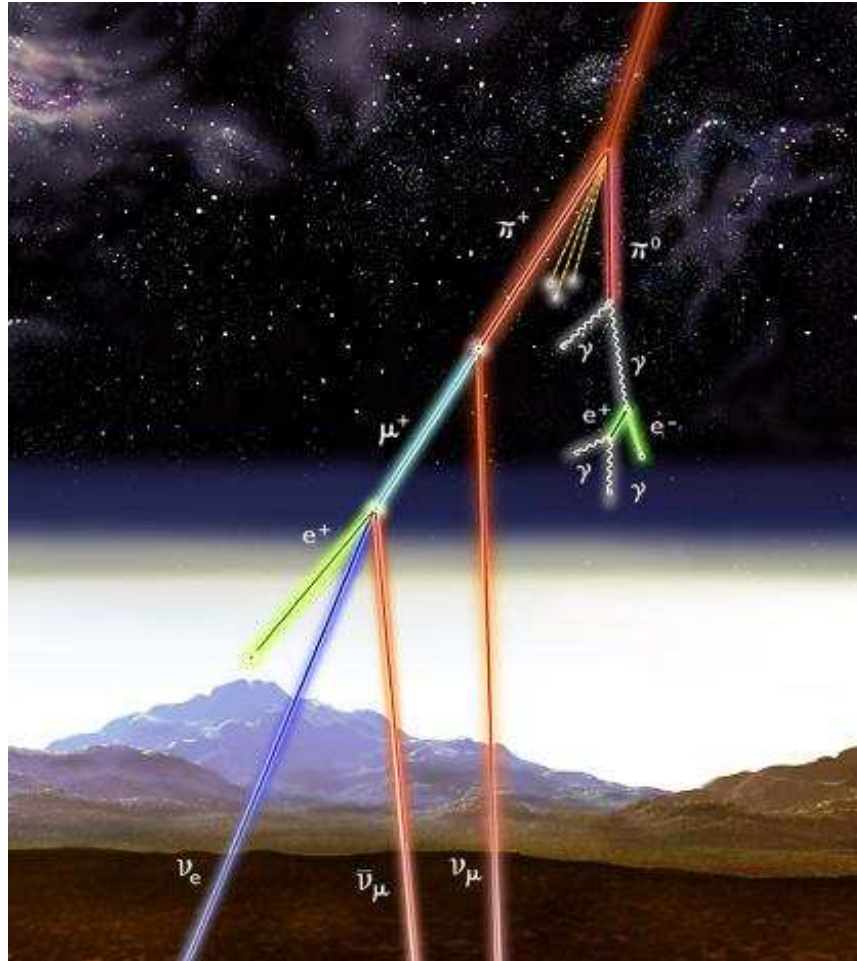


$$\Phi_{^8\text{B}} = 5.05 \times 10^6 \text{ cm}^{-2} \text{ s}^{-1}$$

$$\frac{\Phi_{\text{Hep}}}{\Phi_{^8\text{B}}} \approx 0.16\%$$



# Background induced by Cosmic Rays



## Muon interactions:

Eliminated by muon veto criteria during the events selection

## Atmospheric neutrinos interactions:

Can not be completely removed with muon veto criteria

In order to estimate this background scintillator response to all products of such interactions have to be carefully studied

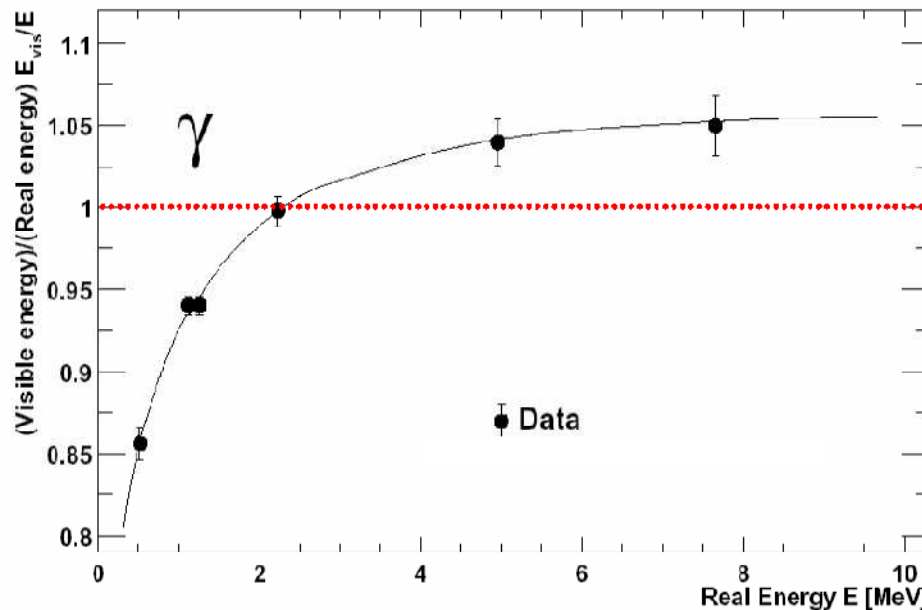
# Scintillator response

For correct interpretation of signals in detector  
it is necessary to know correspondence  
between light output in scintillator and deposit  
energy for all particles

At the early stage of experiment  
collaboration observed strong nonlinear  
behavior of scintillator (quenching) even  
for gammas!

Birks' law:

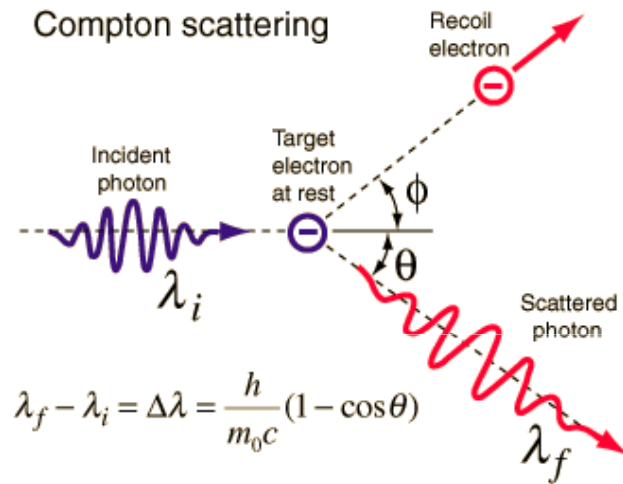
$$\Delta E_{visible} = \frac{\Delta E_{expected}}{1 + k_B (dE / dx)}$$



**Detailed Studies were required!!!**

**We started at UT comprehensive  
program to investigate reasons for  
nonlinear behavior of KamLAND  
scintillator**

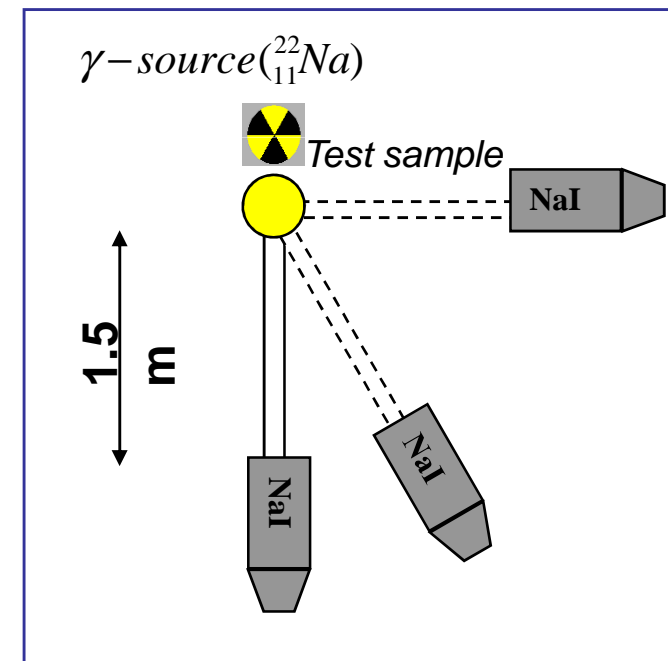
# Response to electrons can be measured using Compton effect



**Energy of recoil electron is determined by scattered photon angle and certain initial energy of the incident photon**

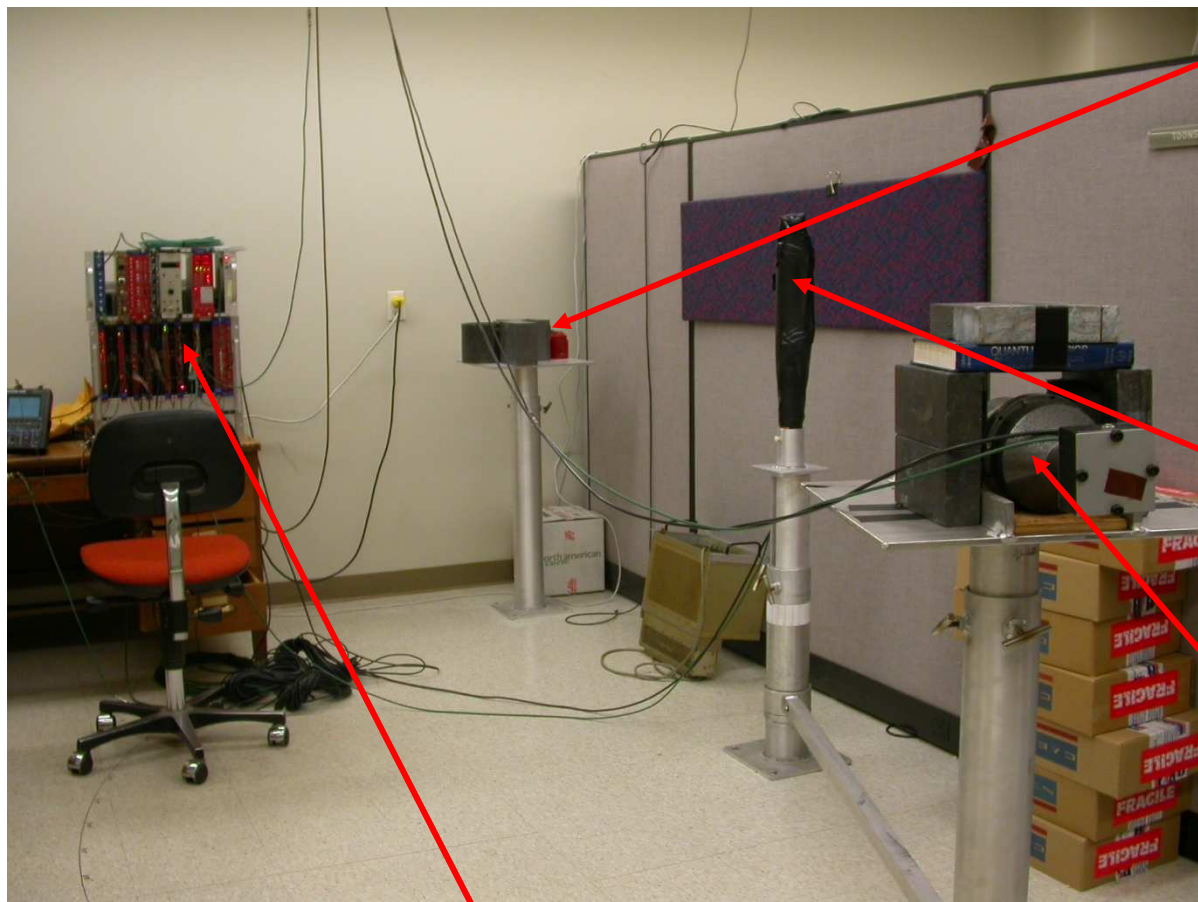
$$E_e^{kin} = E_\gamma - E_\gamma \frac{m_e}{m_e + E_\gamma (1 - \cos\theta)}$$

## Compton spectrometer scheme



**$^{22}\text{Na}$  gamma source  
0.511 MeV and 1.275 MeV**

# Compton Spectrometer Design



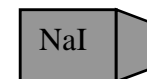
VME DAQ system



1 mCi  $^{22}\text{Na}$  Radiation source with two gamma lines 511 and 1275 keV  
Placed inside massive lead collimator  
 $R_{\text{hole}} = 2.5\text{mm}$   
 $L_{\text{hole}} = 8.5\text{cm}$



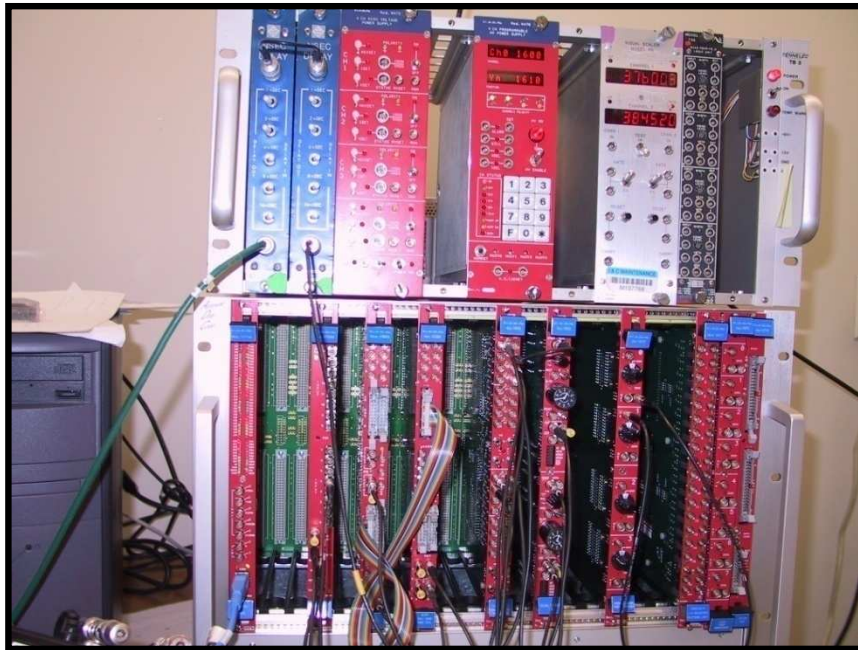
Test sample  
2.5cm radius, 6.35 cm height quartz cylinder



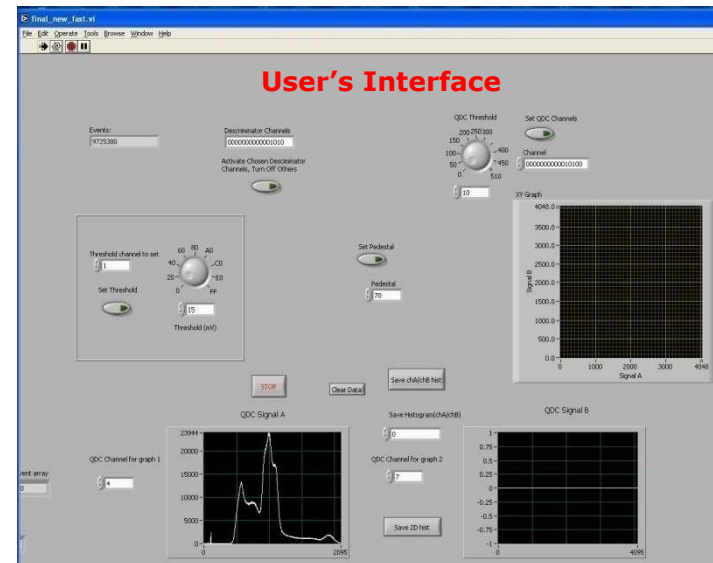
Gamma Detector  $\varnothing 13\text{ cm}$   
With the long 1.6 m arm we have small angular dispersion

# DAQ System

**Crate with VME electronics**



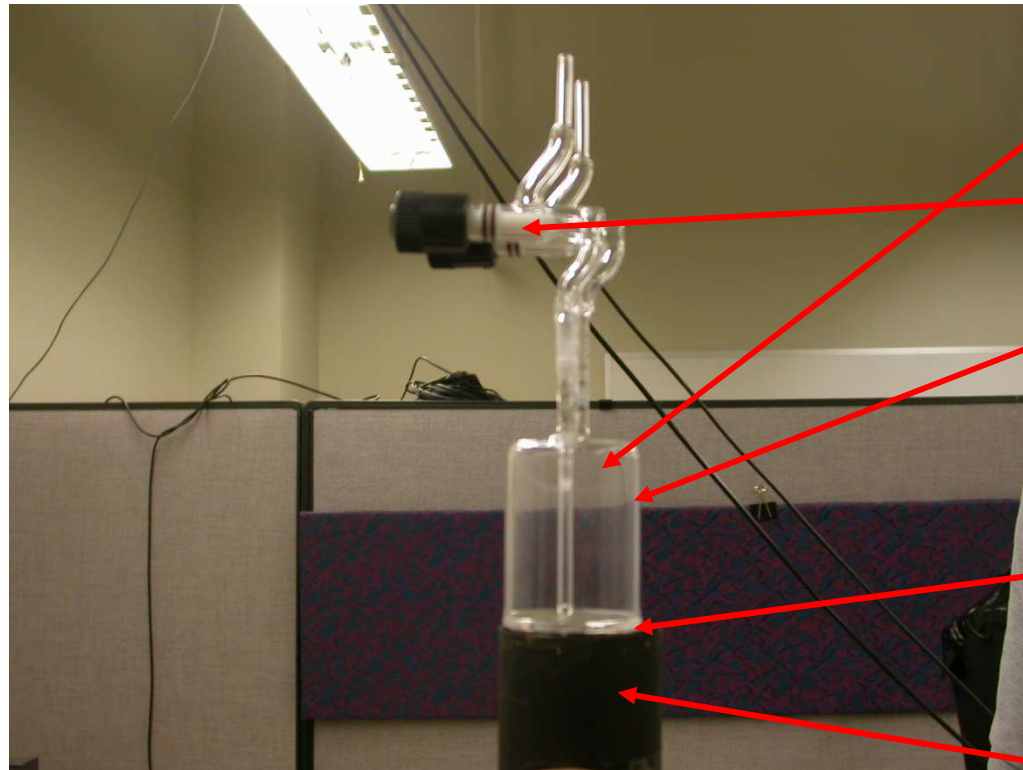
**DAQ software was developed using LabView 7**



**Trigger rate  $\sim 30$  events/min**  
**Rate depend on angular position of NaI, angular acceptance of the spectrometer**



# Target Volume



**KamLAND liquid Scintillator**

**Teflon valves**

**Quartz vessel  
(wrapped in Tyvek)**

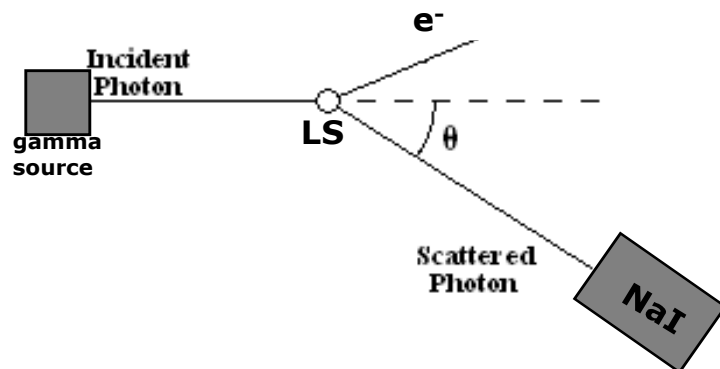
**Bicron Optical Grease**

**Hamamatsu 1161 2" PMT  
with Bialkali photocathode**

**Before measurements scintillator was purged  
with large amount of nitrogen and then vessel  
has been sealed with Teflon valves**

# Spectrometer properties

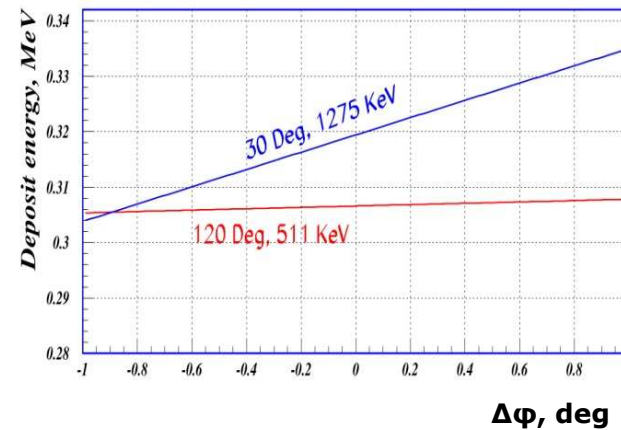
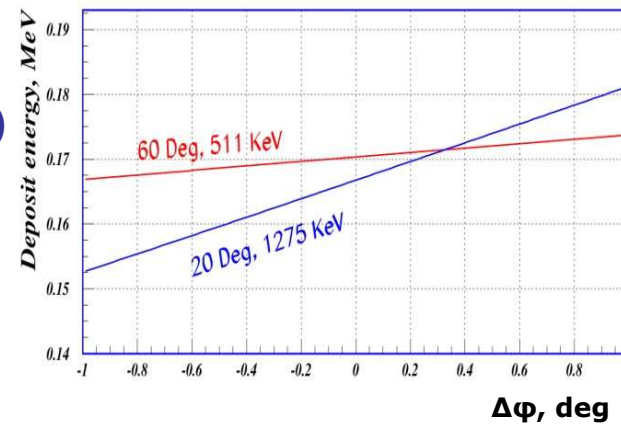
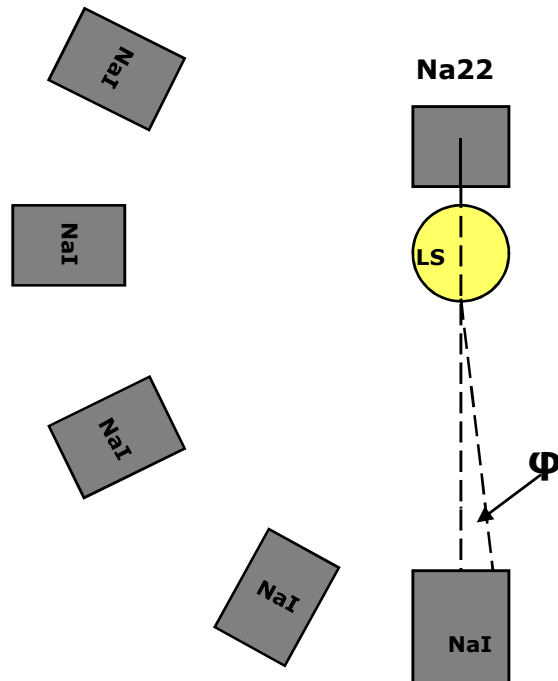
- Selection of the certain deposited energy in the scintillator by electrons is determined by the angular position of the NaI
- Measurements were done from 20 to 120 degrees of scattering angle
- Kinetic energy range for detected electrons is 29-300keV for 511keV gamma line and 166.3-1000keV for 1275keV gamma line
- Alignment of all components of the spectrometer is important part of the experiment (error in determination of the scattering angle can cause the “faked non-linearity”)



$$E_e = E_\gamma - E_\gamma \frac{m_e}{m_e + E_\gamma (1 - \cos \theta)}$$

# Alignment of spectrometer

Scintillator and radiation source position along with the angular scale were aligned using theodolite (accuracy is better than 0.1 degrees)

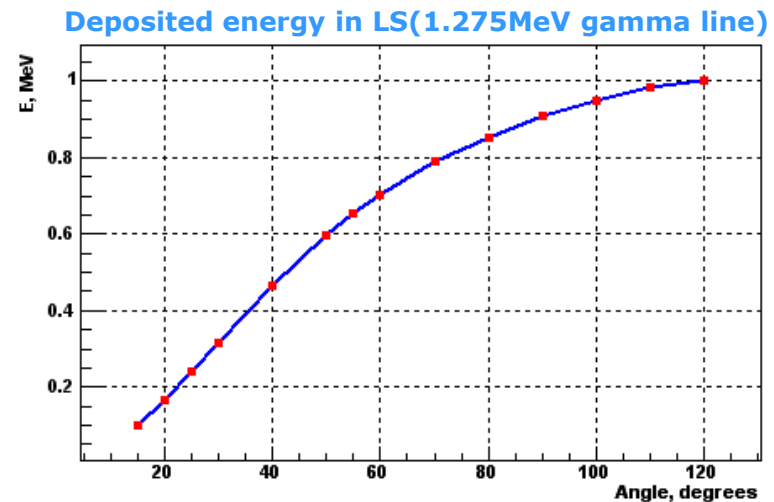
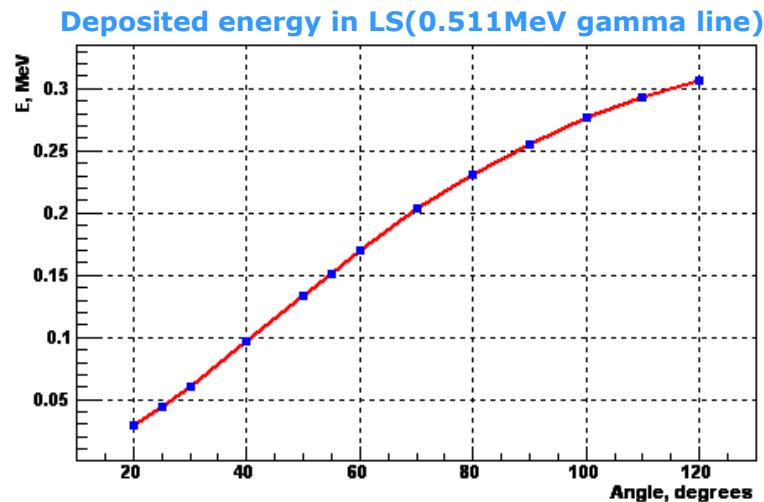


Deviation of real angle from what we think it is

1 degree misalignment can cause up to 10% non-linearity

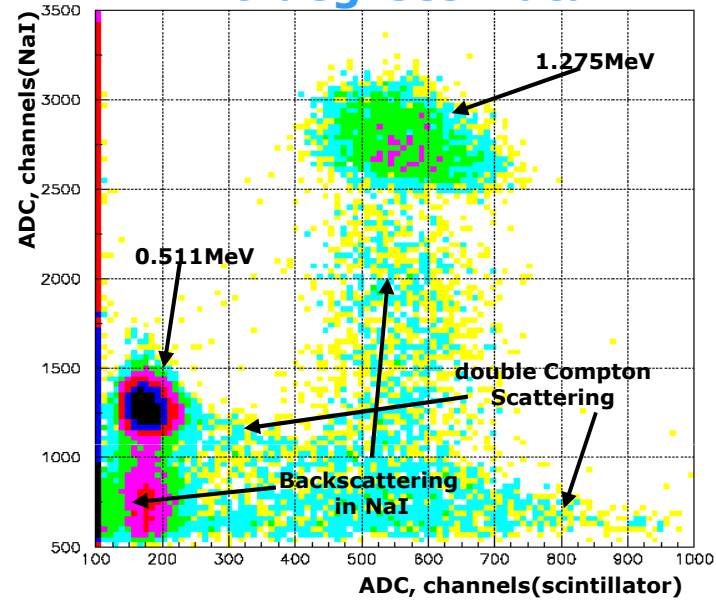
# Energy deposition Monte-Carlo simulation (without quenching)

- Monte-Carlo simulation was made using GEANT
- Physical and geometrical properties of the spectrometer were described in order to define energy deposition in liquid scintillator
- Errors of energy deposition are about 0.2%
- Difference in the energy deposition in LS between MC and Compton Formula is up to 0.9%

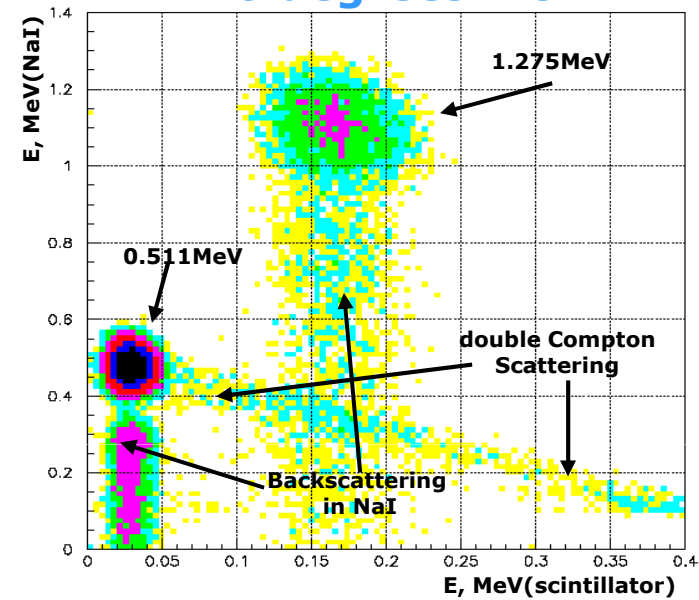


# Data & Monte-Carlo

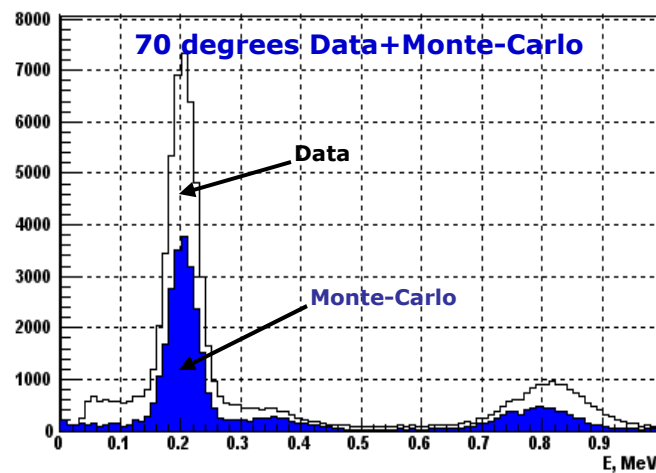
## 20 degrees Data



## 20 degrees MC

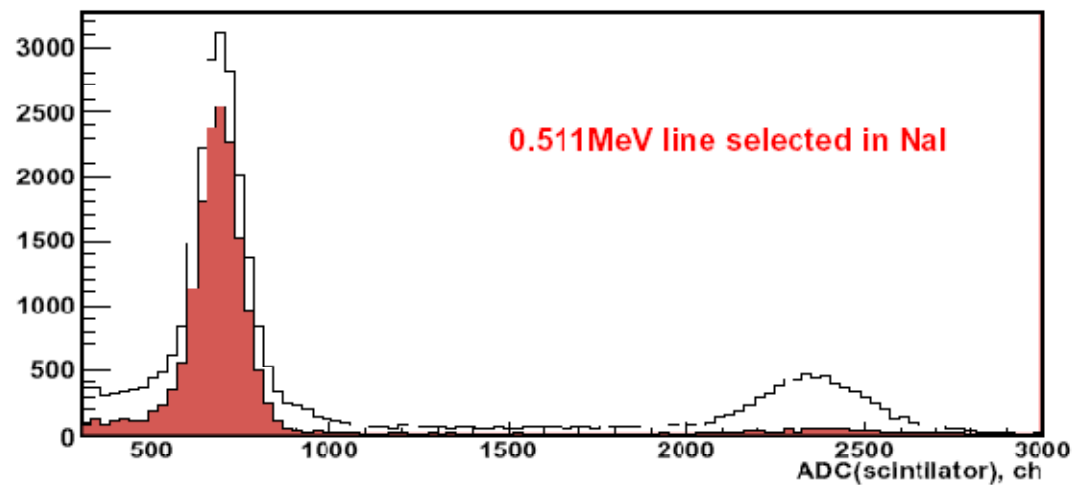


## 70 degrees Data+Monte-Carlo

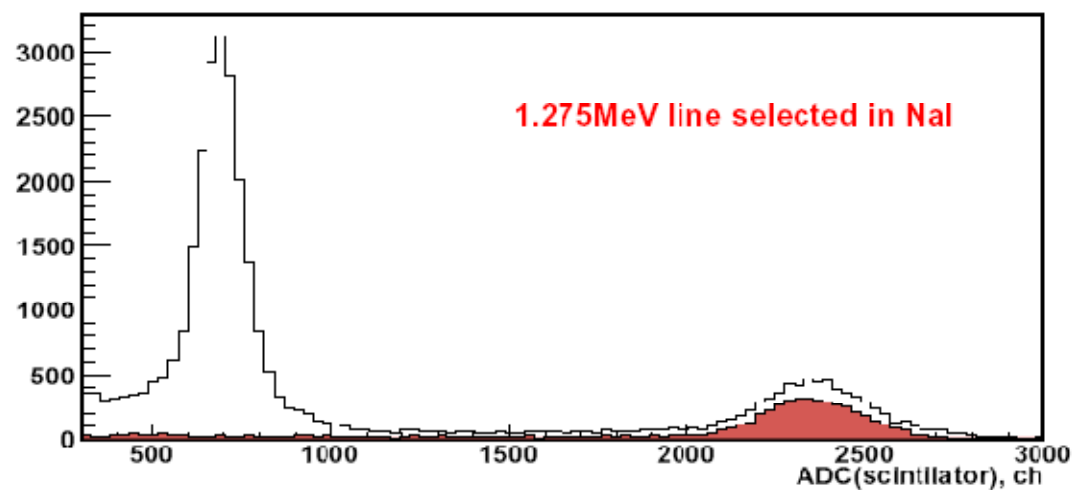




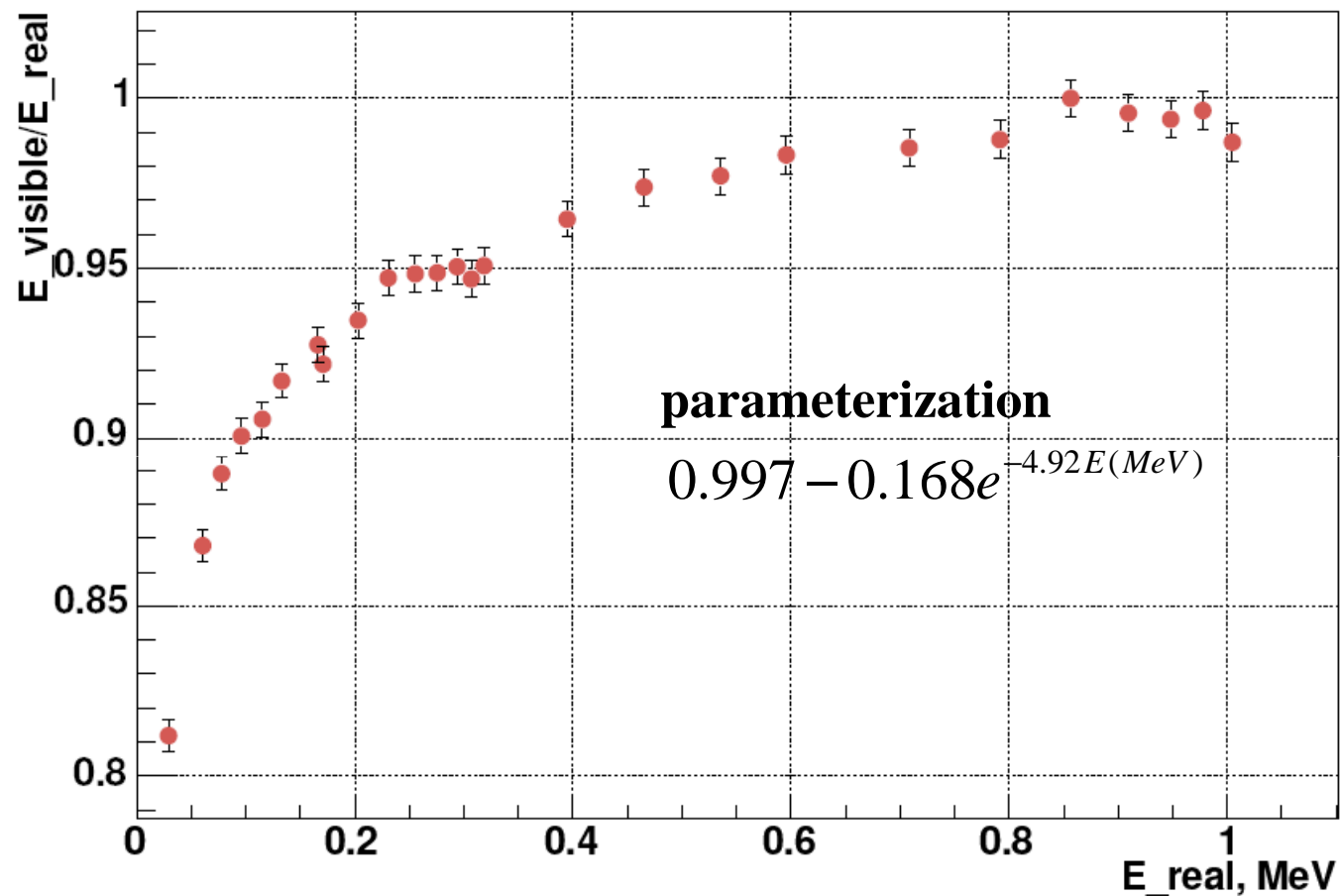
# Event selection in Scintillator



**Energy cut in NaI let  
us clearly select  
Compton scattering in  
the test sample for  
both gamma lines**

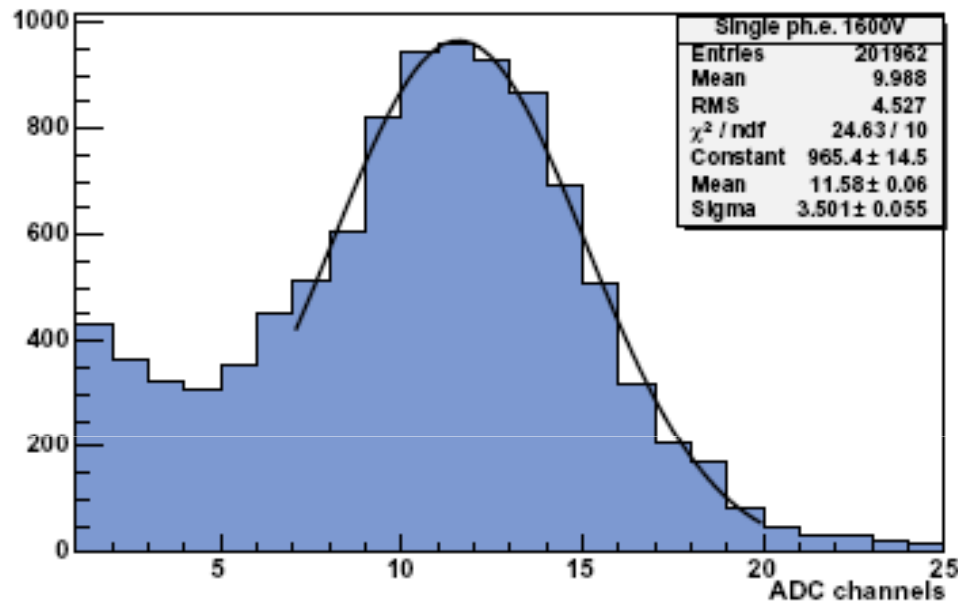


# KamLAND LS response to electrons



Systematic errors 0.5%

# Scintillator Light output calibration



**1ph.e.=0.001554MeV**

**N=643.5+/-3.8 ph.e./MeV**

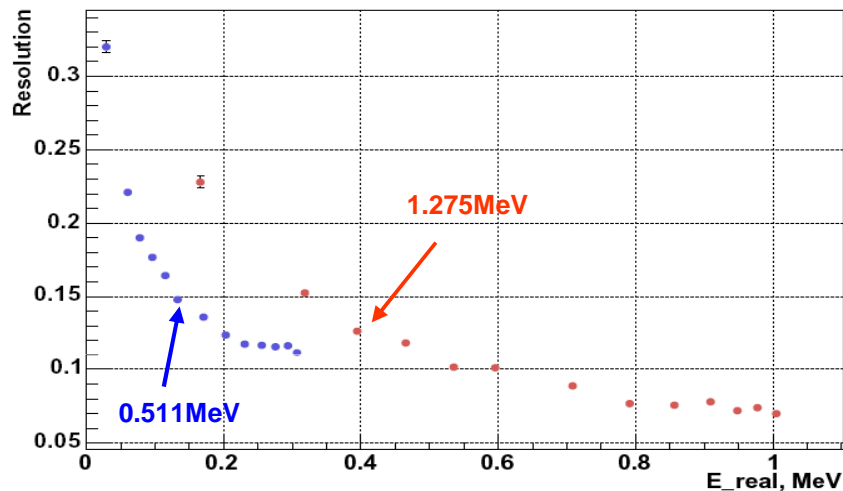
Since the single photoelectron has its own resolution it gives additional contribution to the final photo-statistic resolution

$$\frac{\delta N}{N} = \sqrt{\frac{1 + \alpha^2}{N}} = \frac{1.0447}{\sqrt{N}}, \alpha = 0.3 - \text{Single ph.e. resolution}$$

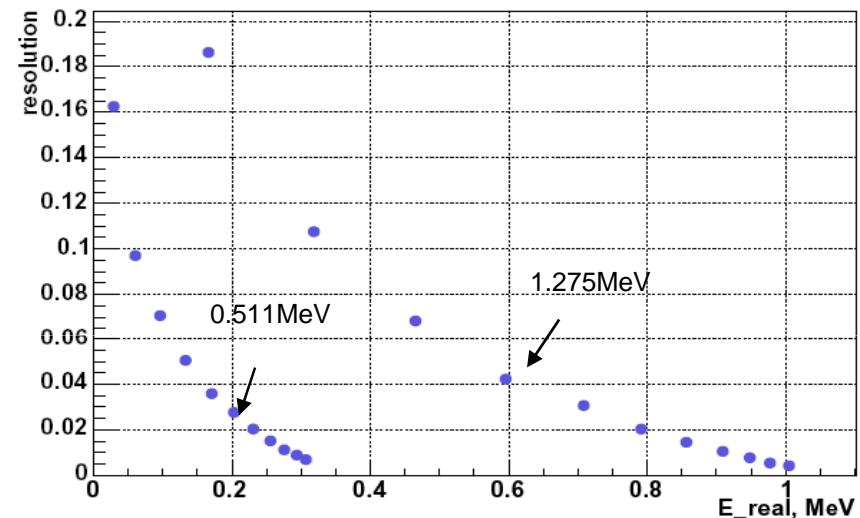
# Spectrometer Resolution

**Spectrometer Resolution consists of two components: pure energy resolution and energy resolution due to angular dispersion**

## Spectrometer Resolution (real data)



## Energy resolution due to angular dispersion (Monte-Carlo)



## Extracted Energy Resolution

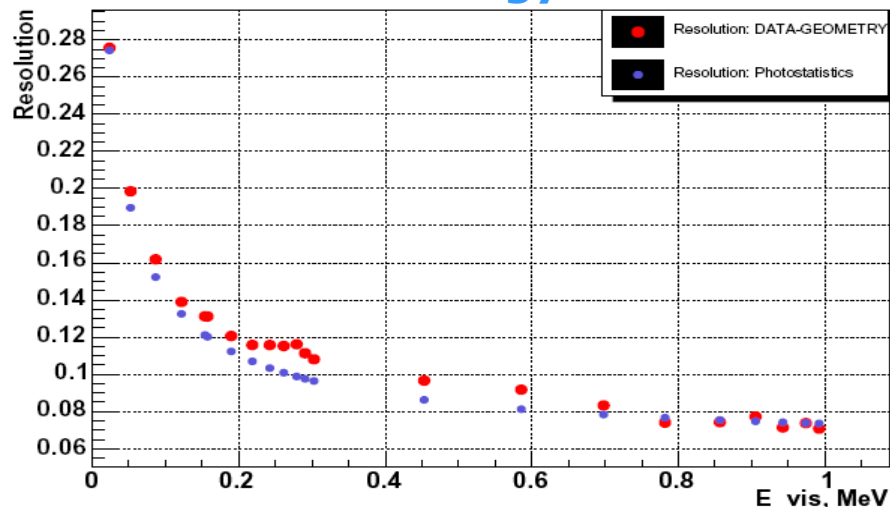


**Photo-statistic resolution plus constant term (light collection uniformity)**

$$\frac{\delta E}{E} = \sqrt{(0.061)^2 + \frac{(1.0447)^2}{N_{\text{ph.e.}}}}$$

**Photo-statistic resolution was taken from calibration using single ph.e.**

# Monte-Carlo study (non-linearity)

**We decided to perform M.C. study to understand which physical processes can explain this non-linearity.**

- Calculate Cherenkov contribution in photoelectrons exactly (emission, reemission, tracking, QE, etc.)
- Simulate energy deposition with different Birks coefficients
- Mix Scintillation and Cherenkov light using parameter  $N$  photoelectrons from scintillation per MeV

Conversion Ph.e. to the Signal from PMT

Conversion deposit energy into Ph.e.

$$E_{\text{vis}} = k \cdot (E_{\text{dep}}(E) \cdot m + N_{\text{Ch}}(E))$$

Calculated in GEANT, Birks dependent

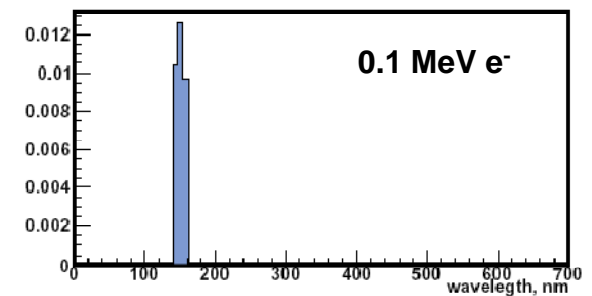
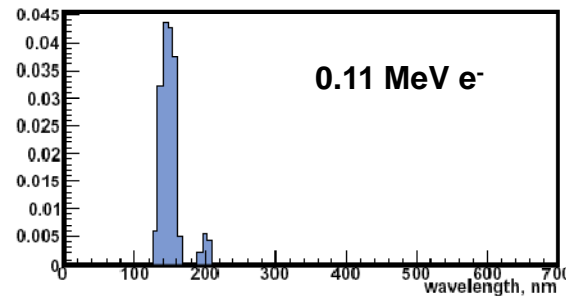
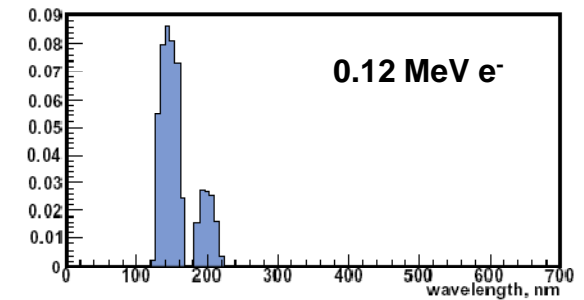
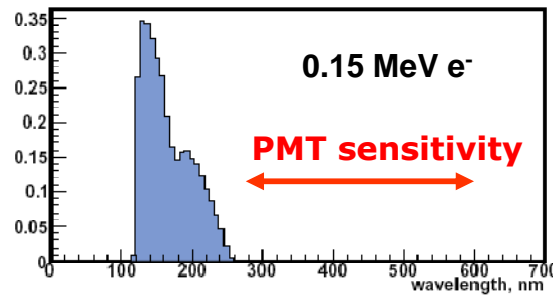
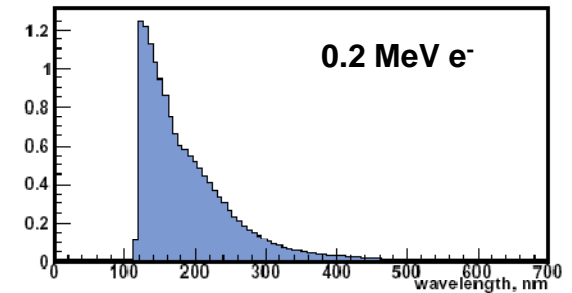
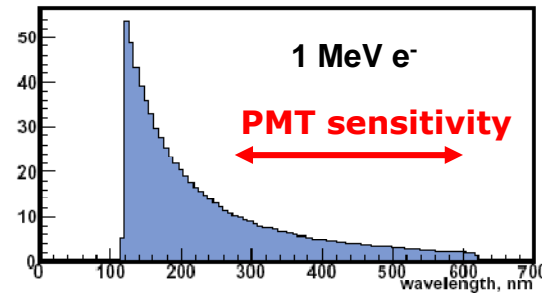
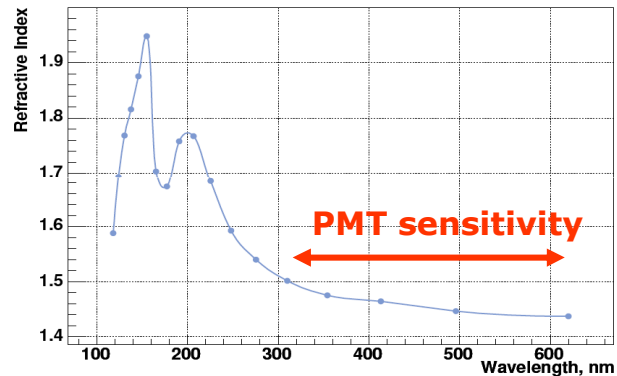
Calculated in GEANT with reemission



# Cherenkov Photons Production

$$\frac{d^2 N}{dx d\lambda} = \frac{2\pi\alpha z^2}{\lambda^2} \left[ 1 - \frac{1}{\beta^2 n^2(\lambda)} \right]$$

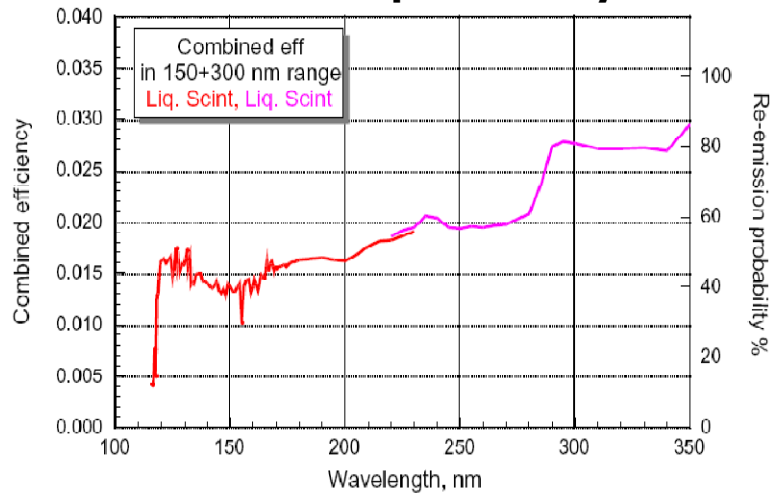
Reconstructed refractive index for  
KamLAND LS



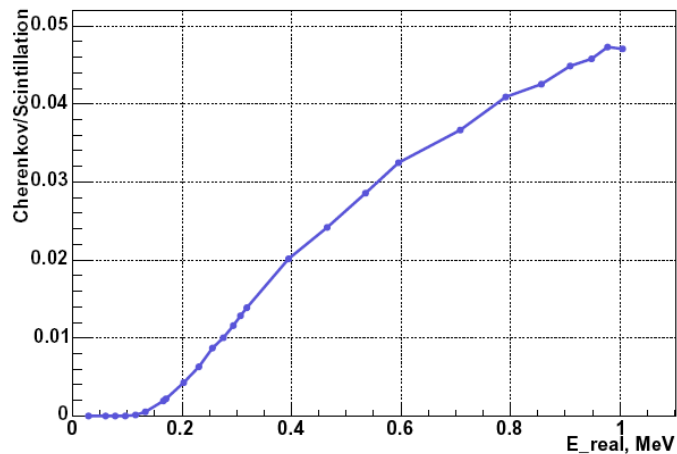
All plots normalized to one incident electron

# Cherenkov Light Production + Reemission (Monte-Carlo)

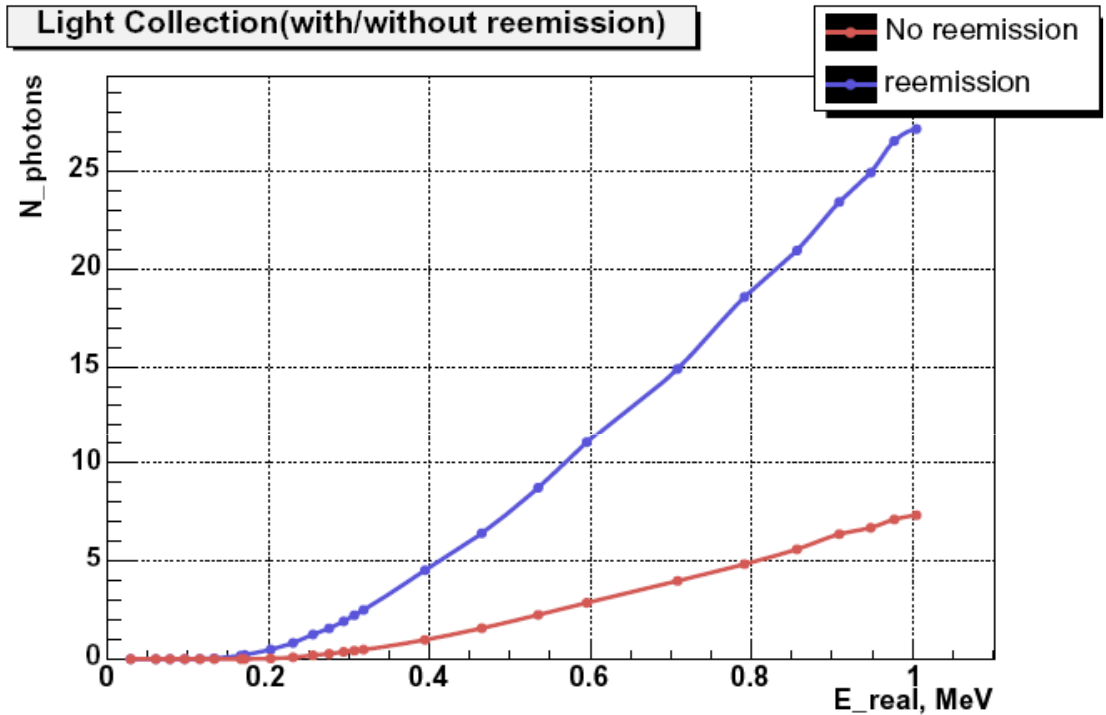
## Reemission probability



## Cherenkov light contribution



## Light Collection(with/without reemission)

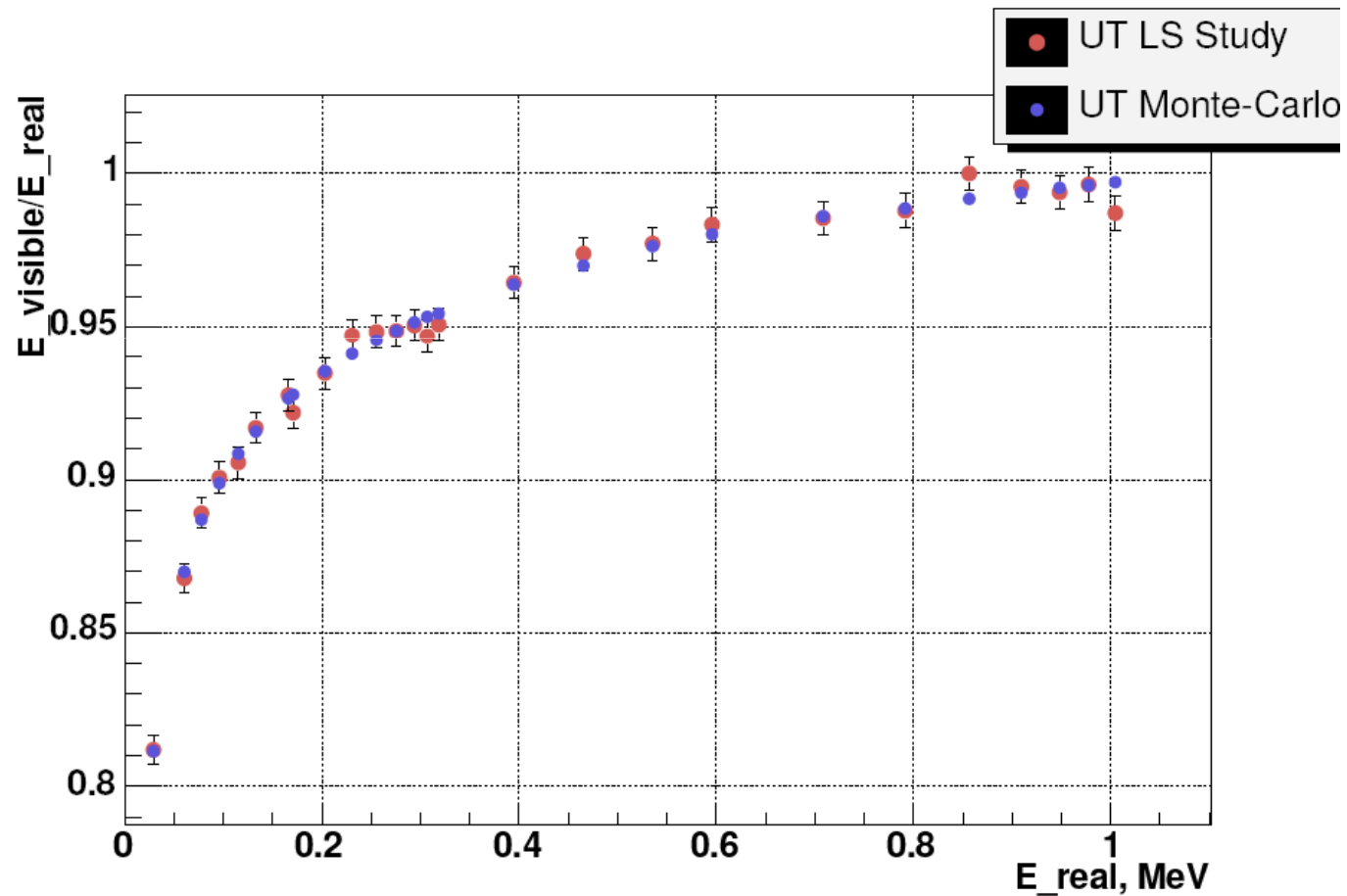


Reemission increased number of Cherenkov photons detected at 1 MeV by factor of 3.7

Cherenkov light contribution to the total light yield is 4.5% at 1MeV

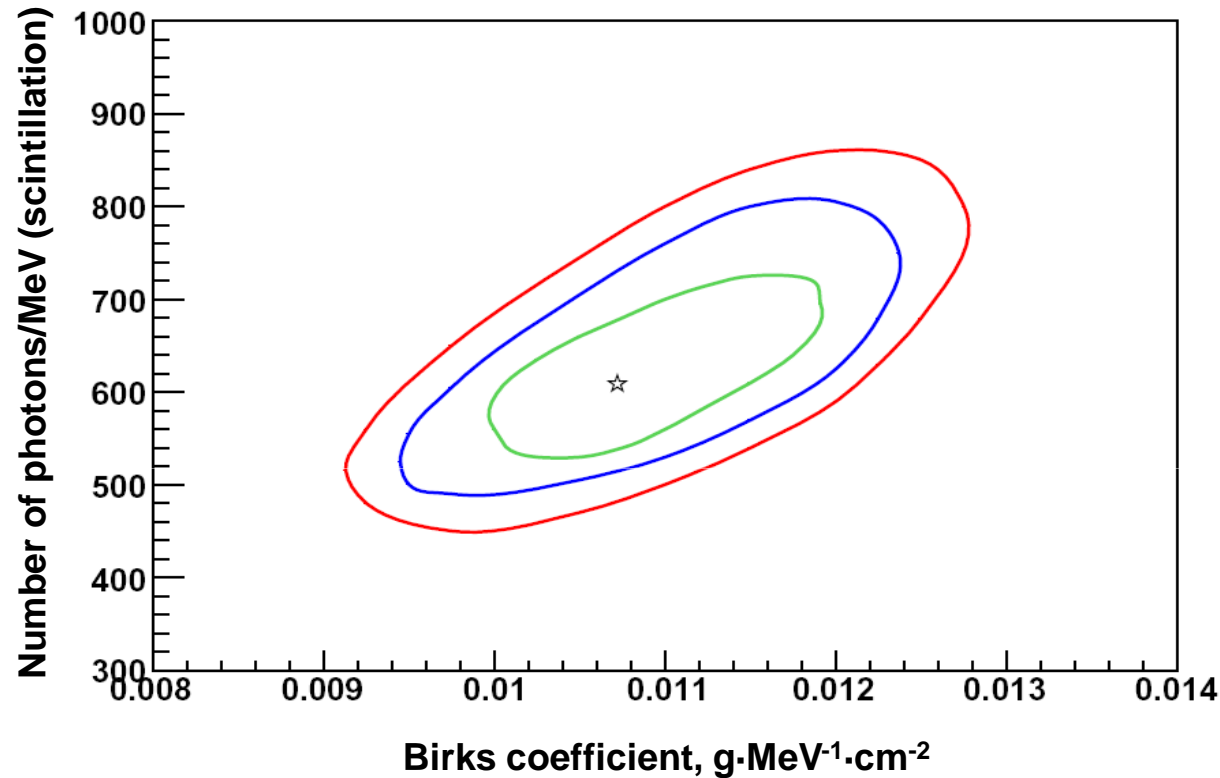
# Data vs. M.C.

Variation of Birks coefficient and Scintillation light output was made to obtain the same shape of nonlinearity measured with Compton Spectrometer  
Cherenkov light output has been calculated and fixed



Very good agreement between data and M.C.

## Best fit (Monte-Carlo)



**N ph.e /MeV best fit is  
609 ph.e./MeV**

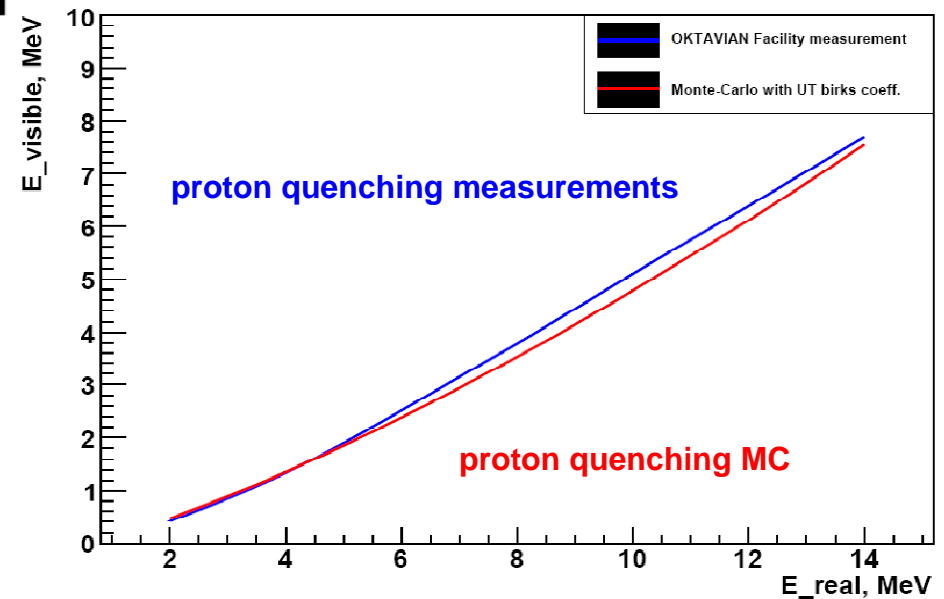
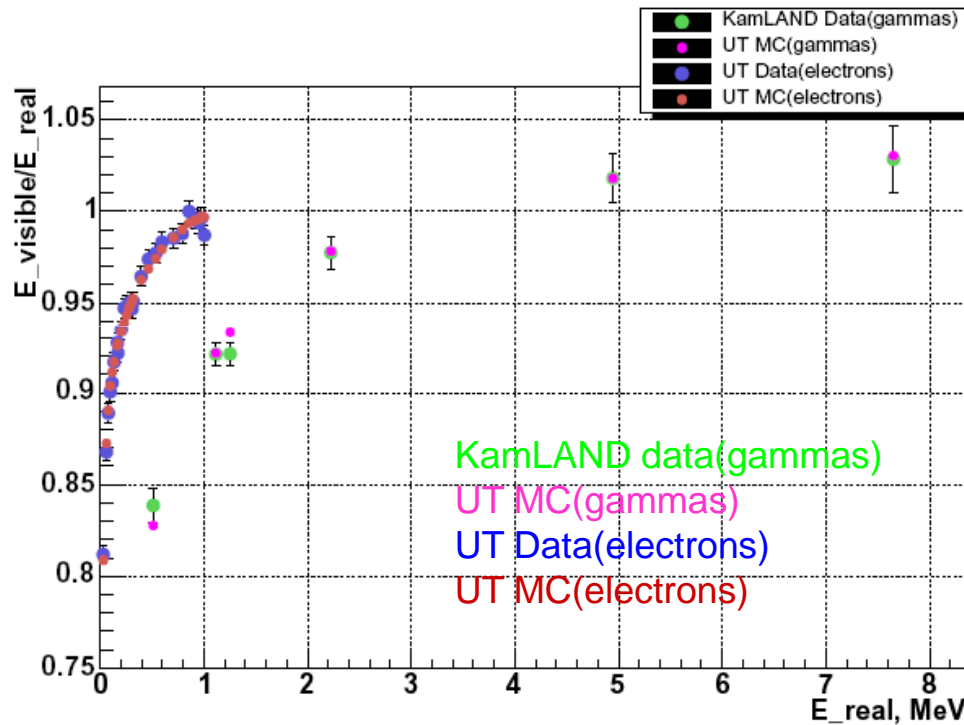
**Good agreement with  
direct measurement (single ph.e.)  
N ph.e./MeV=643.5+/-3.8 ph.e.**

**Our best Birks value is  
0.01072 g/(MeV·cm<sup>2</sup>)  
=0.138mm/MeV**

**GEANT recommended  
K<sub>B</sub>=0.013g/(MeV·cm<sup>2</sup>)**

# Comparison with Gammas and Protons

Current model, optimized on electrons with  $E < 1$  MeV, was applied to calculate LS response to gammas and protons

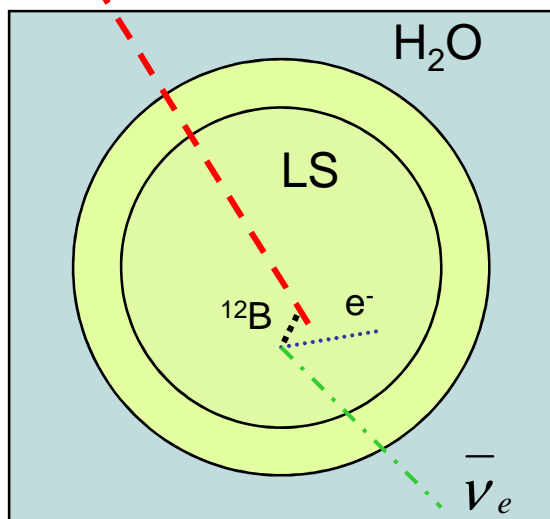


MC, developed to explain nonlinear behavior of scintillator for electrons reproduces well nonlinearity for gammas and protons!!!



# Energy reconstruction ( $^{12}\text{B}$ events)

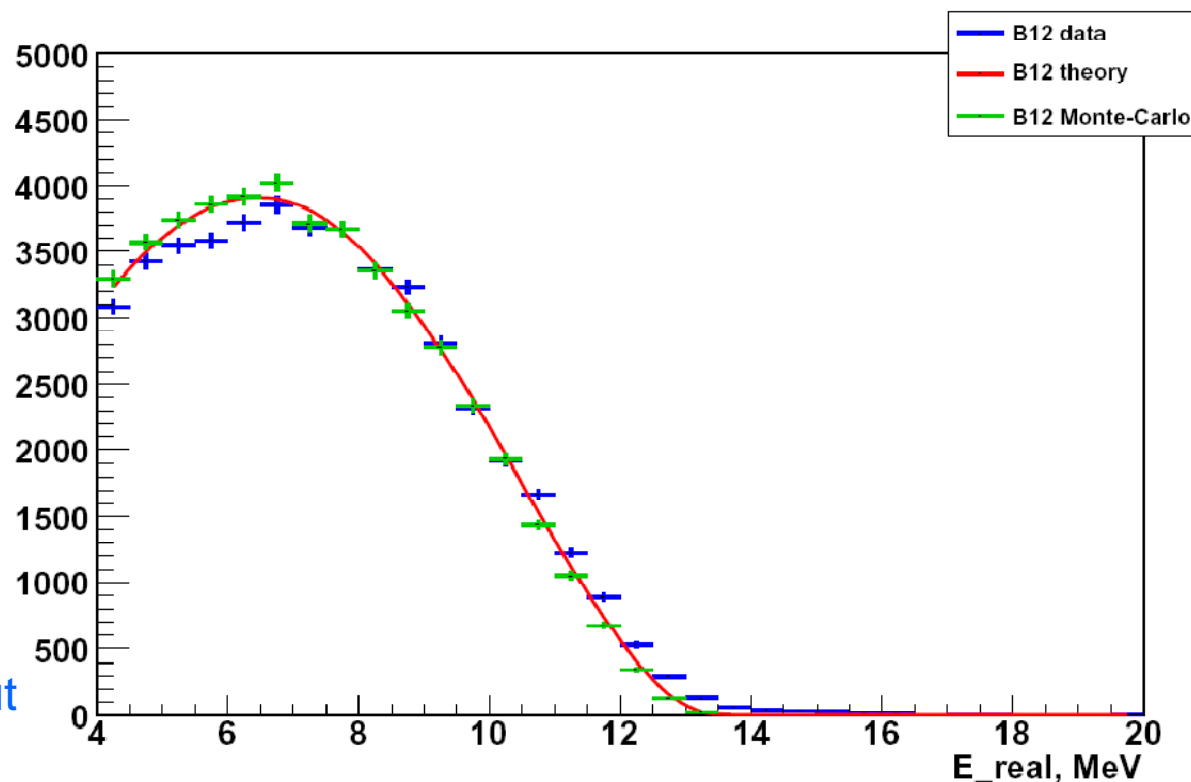
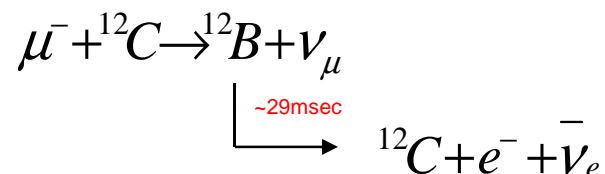
$\mu$  **All KamLAND calibration sources have energies below 8MeV**



After muon signal the events  
have been selected during  
2-60msec

Background off-timing  
window 502-560msec

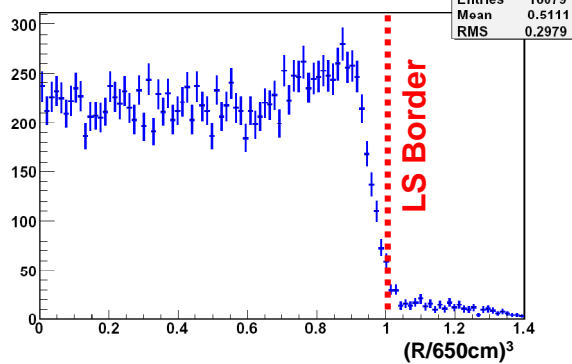
Distance from muon track cut  
 $dL < 300\text{cm}$



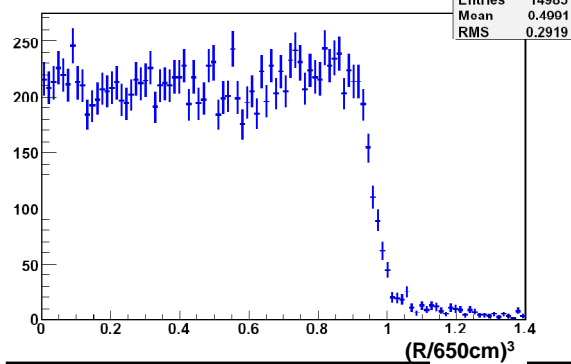
**Energy in the interval of  $7.5 < \text{MeV} < 14$  reconstructed reasonably well**

# Vertex Reconstruction ( $^{12}\text{B}$ events)

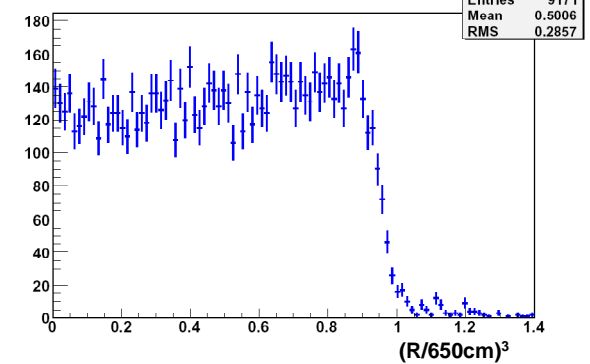
B12 Spacial Distribution  $5\text{MeV} < E < 7\text{MeV}$



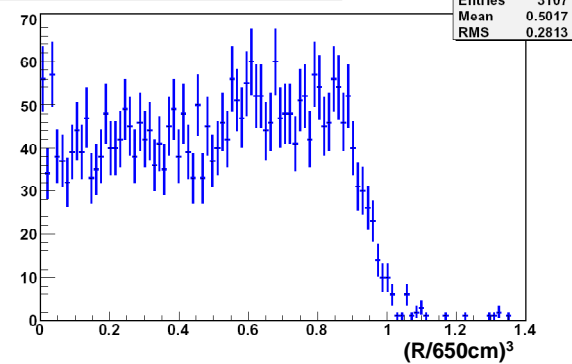
B12 Spacial Distribution  $7 < E < 9\text{MeV}$



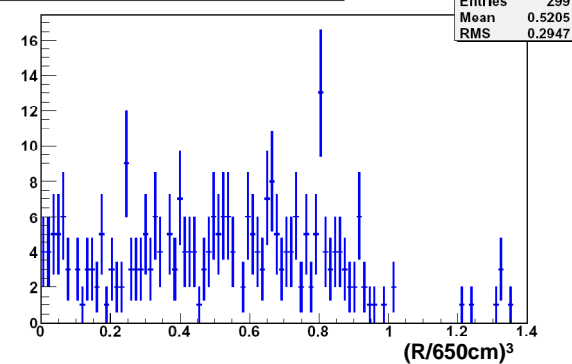
B12 Spacial Distribution  $9 < E < 11\text{MeV}$



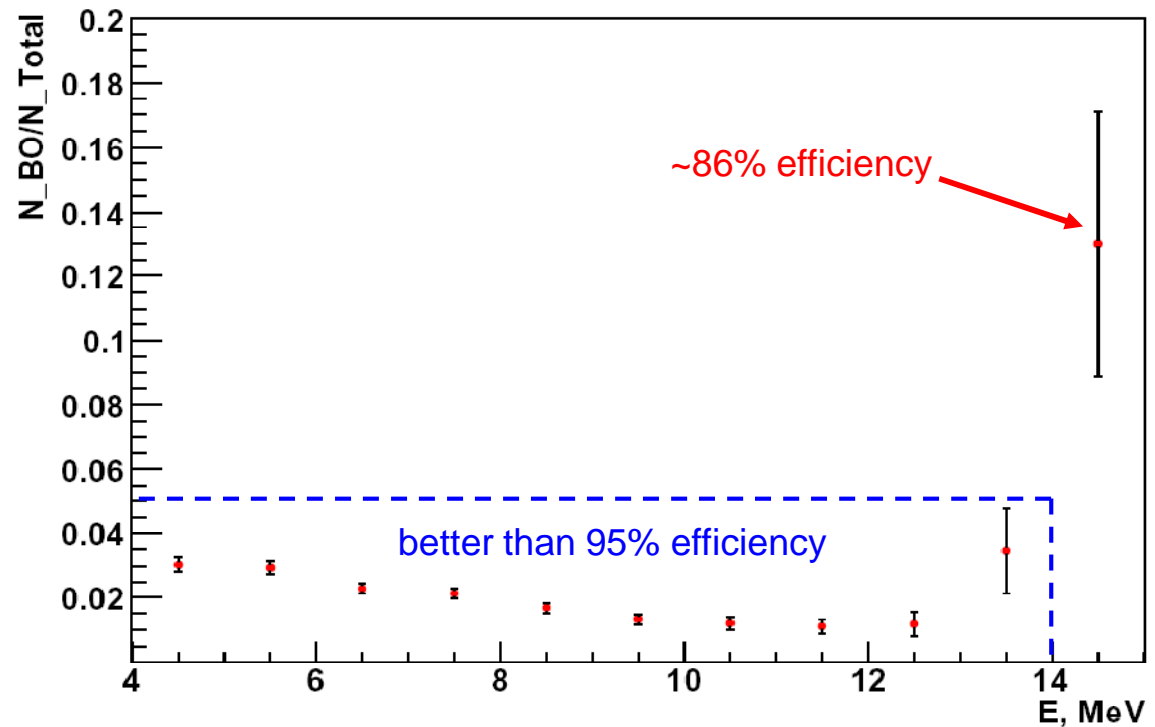
B12 Spacial Distribution  $11 < E < 13\text{MeV}$



B12 Spacial Distribution  $13 < E < 15\text{MeV}$



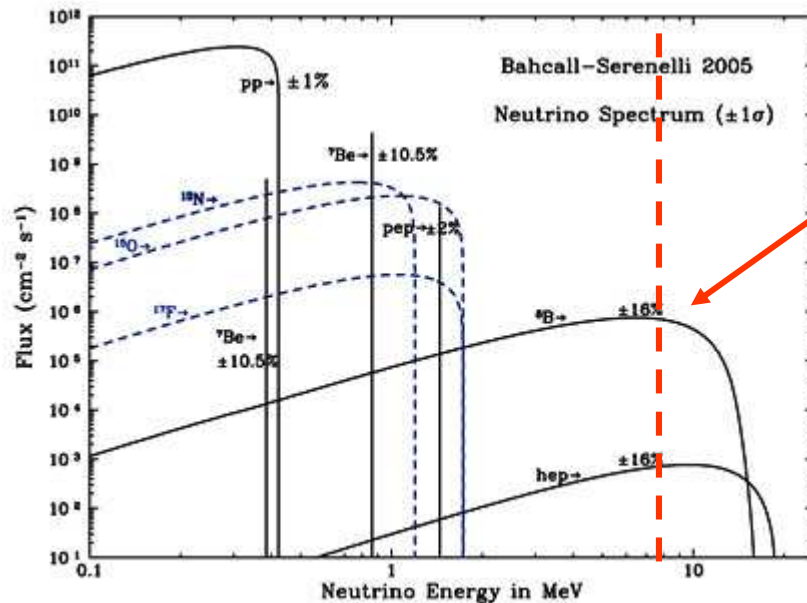
B12 recontruction inefficiency



# Solar antineutrino analysis

- Previous result
- Electron antineutrino candidates selection
- Background calculations

# Search for Solar Antineutrinos (old KamLAND result)

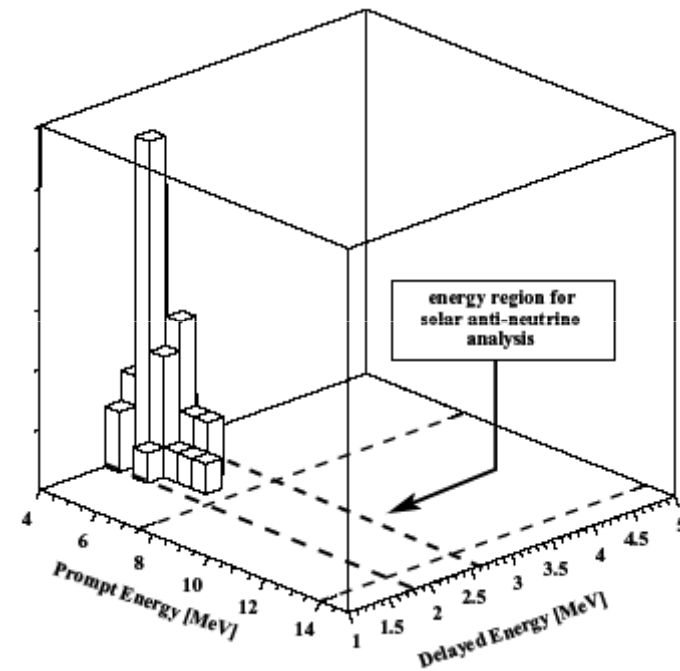


The tail from reactor antineutrinos is visible below 7.5 MeV

Current KamLAND limit on  
Solar electron antineutrino flux:  
 $\Phi < 3.7 \times 10^2 \text{ cm}^{-2} \text{s}^{-1}$   
Or neutrino conversion probability:  
 $P < 2.8 \times 10^{-4}$

This limit can be improved with larger in-hands statistics

${}^8\text{B}$  solar  $\nu_e$  can transform to  
anti- $\nu_e$  in solar magnetic field  
Phys. Rev. Lett. 92:071301, 2004



Energy distribution of event candidates  
after 185.5 days(0.28 ton-year)  
**0 candidates have been found**

# High Energy Candidates Selection

## Muon criteria:

**TotalCharge17 > 10000 p.e. or  
(TotalCharge17 > 500 p.e. & N2000D > 5)**

## Veto:

Low charge muon

**(TotalCharge17 < 40000 p.e.)**

**2msec veto for whole volume of the detector  
(TotalCharge17 > 13000 p.e.)**

Energetic muon (showering muon)

**(TotalCharge17 > 40000 p.e. & dQ > 10<sup>6</sup> p.e.)**

**2sec veto for whole volume of the detector**

Miss reconstructed muon

**(TotalCharge17 > 40000 p.e. & badness > 100)**

**2sec veto for whole volume of the detector**

Well reconstructed non-energetic (non-showering) muon

**(TotalCharge17 > 40000 p.e. & badness < 100 & dQ < 10<sup>6</sup> p.e.)**

**2msec veto for whole volume of the detector**

**2sec veto around the muon track within  
3m(delayed only)**

## Spacial & Energy Cuts:

$R_{\text{prompt}}, R_{\text{delayed}} < 600 \text{ cm}$

$|R_{\text{prompt}} - R_{\text{delayed}}| < 160 \text{ cm}$

$dT < 1000 \mu\text{sec}$

$7.5 \text{ MeV} < E_{\text{prompt}}(\text{real}) < 30 \text{ MeV}$

$1.8 \text{ MeV} < E_{\text{delayed}}(\text{visible}) < 2.6 \text{ MeV}$

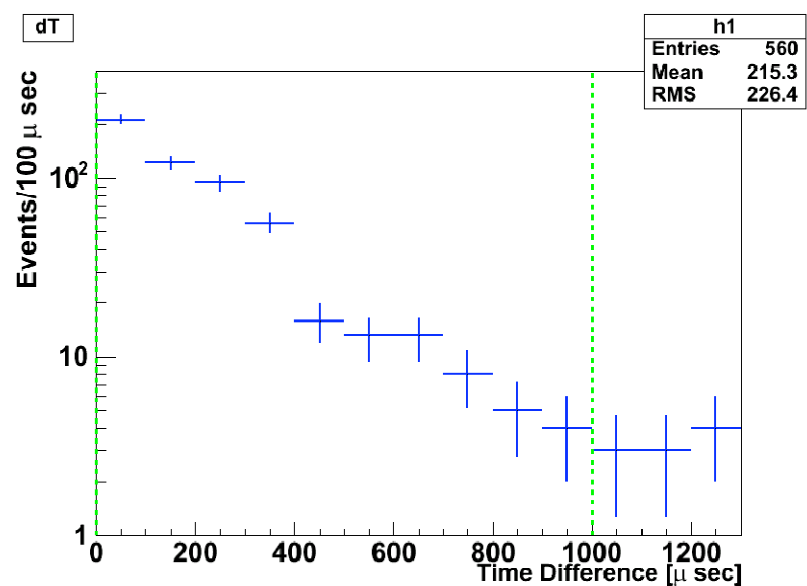
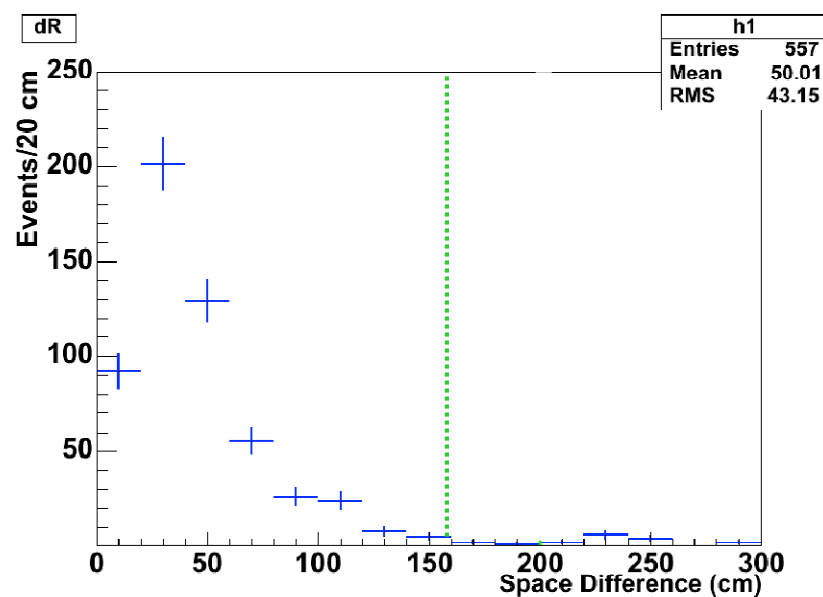
## Improvement: Statistics

**Livetime** **×7.7 statistics**  
**185.5 days → 1425.9 days**

**New energy and muon fitters**  
**New vertex reconstruction tool**  
**New event selection criteria**

$$dQ = Q_{\text{ID}} - Q_{\mu \text{ track}}$$

# Spatial & Time Correlation between prompt and delayed



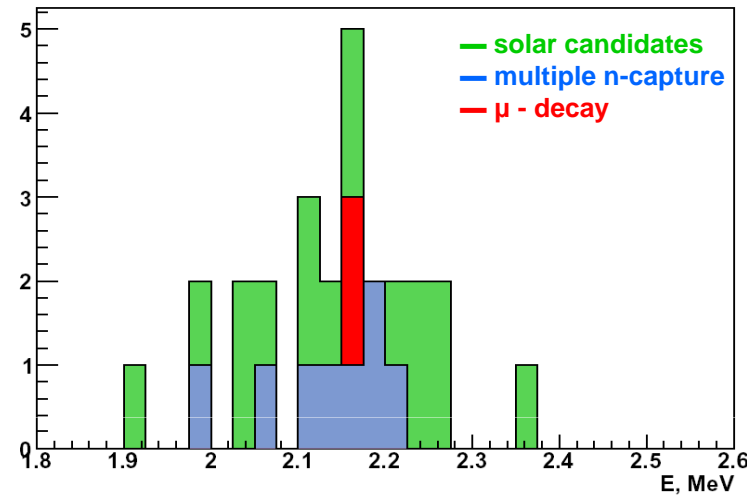
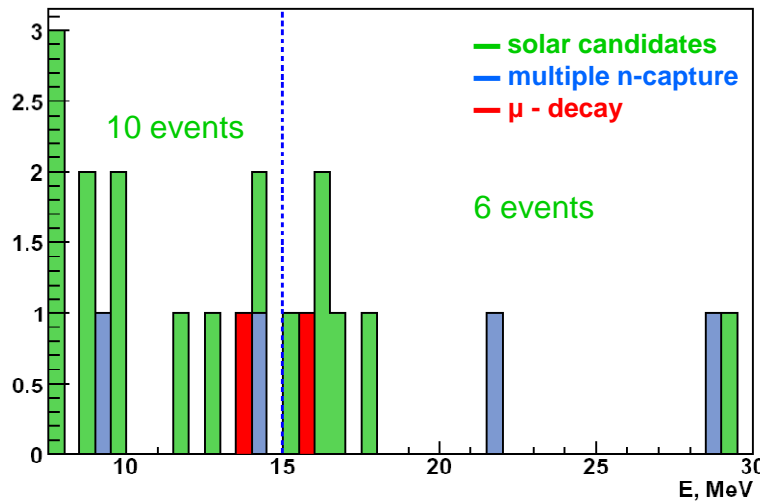
Plots were made for reactor antineutrino candidates

# High Energy Candidates 6.0m fiducial volume

solar antineutrino  
energy range

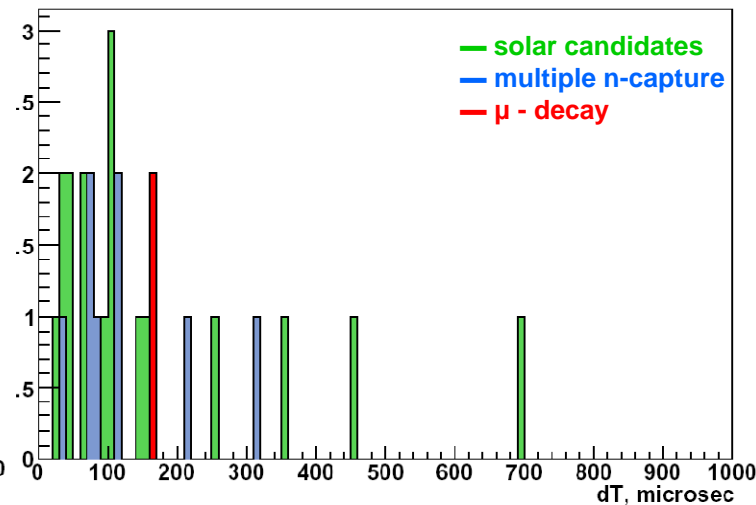
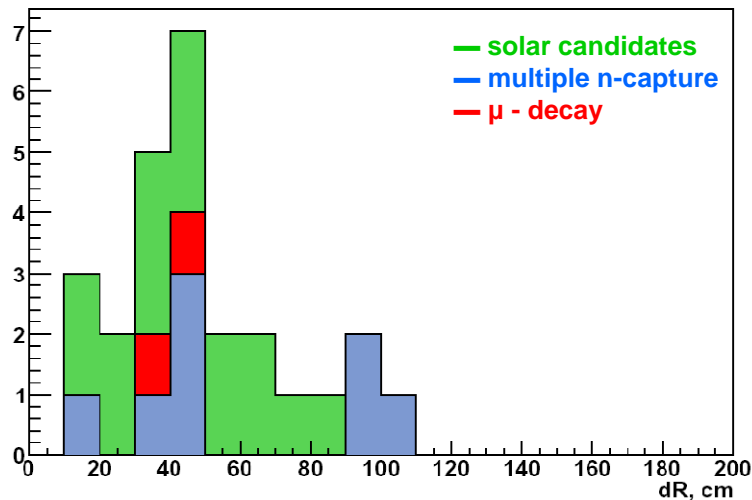
$E_{\text{prompt}}$

$E_{\text{delayed}}$



$\Delta R$

$\Delta T$



7.5->15MeV:  
10 candidates has  
been selected

+

2 triple coincidence:  
multiple neutrons  
capture  
Run# 1824, Prompt#  
13658585  
Delayed# 13658586,  
13658587  
Run# 5941, Prompt#  
4644789  
Delayed# 4644790,  
4644791

+

1 muon decay  
(triple coincidence)

Run# 5380  
Prompt\_1#  
41470(muon,  
 $E=15.5\text{MeV}$ )  
Prompt\_2#  
41471(positron,  
 $E=13.6\text{MeV}$ )  
Delayed# 41472  
 $dT_{1-2}=1.23\mu\text{sec}$   
 $dR_{1-2}=6.4\text{ cm}$

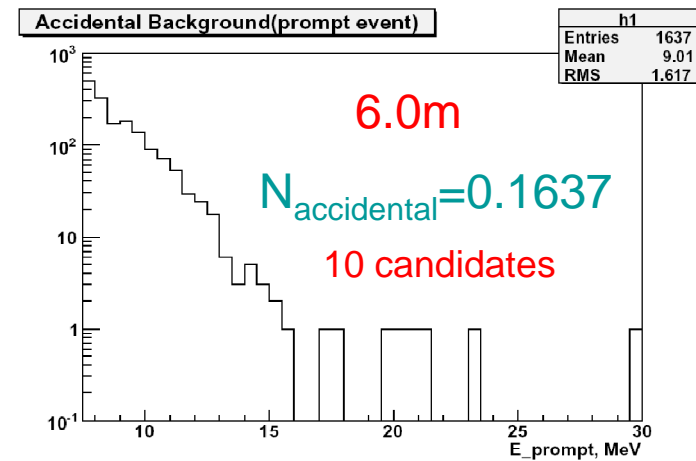
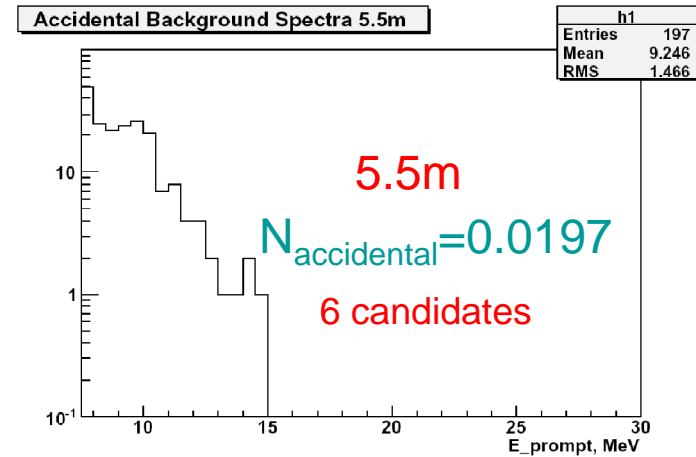
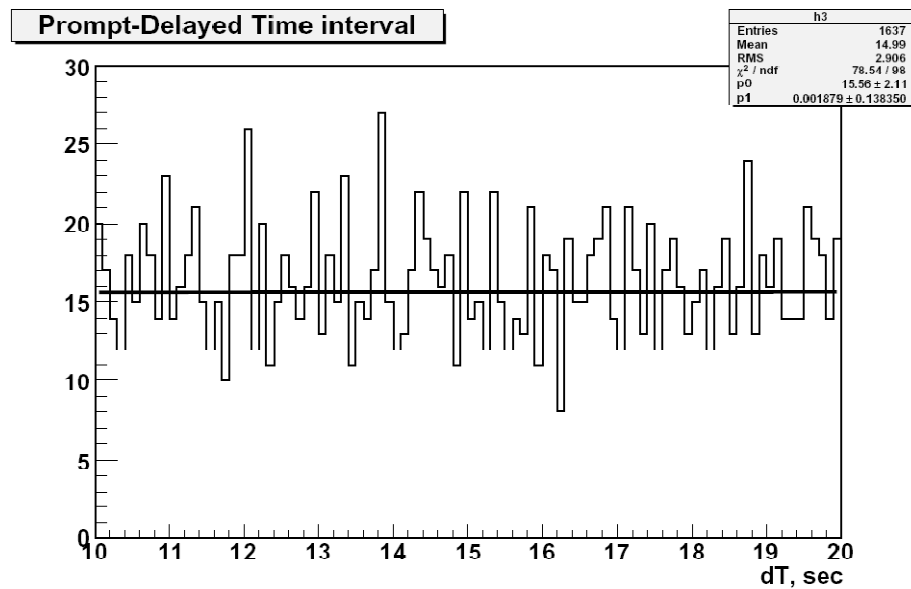


## Background sources

- Accidental Background
- $^9\text{Li}$  produced by cosmic muons
- Reactor antineutrinos
- Background from atmospheric neutrinos

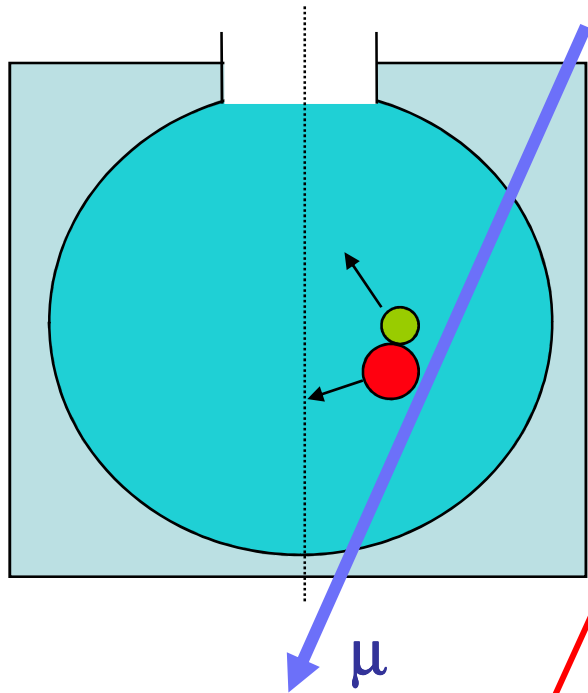
# Accidental Background

Delayed events time window:  $10.005\text{sec} < dT < 20\text{sec}$  from Prompt event  
 $10^4$  scaling factor to delayed events time window in analysis



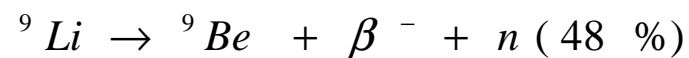
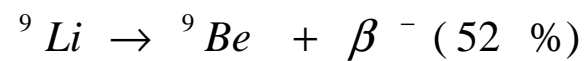
Accidental background is negligible

# Spallation Products



Isotope	Half-Life	Endpoint	Decay Type
$^{12}\text{N}$	0.011 s	17.4 MeV	$e^+$
$^{13}\text{B}$	0.017 s	13.4 MeV	$e^-$
$^{12}\text{B}$	0.0202 s	13.4 MeV	$e^-$
$^{11}\text{Li}$	0.09 s	16.0 MeV	$e^-$
$^8\text{He}$	0.12 s	10.6 MeV	$e^-$ with n
$^9\text{C}$	0.13 s	16.0 MeV	$e^+$ with p or $\alpha$
$^9\text{Li}$	0.18 s	13.6 MeV	$e^-$ with n
$^8\text{B}$	0.77 s	17.97 MeV	$e^+$ with $\alpha$
$^6\text{He}$	0.81 s	3.5 MeV	$e^-$
$^8\text{Li}$	0.84 s	16.0 MeV	$e^-$ with $\alpha$
$^{16}\text{N}$	7.1 s	10.4 MeV	$e^-$
$^{11}\text{Be}$	13.8 s	11.5 MeV	$e^-$ with $\alpha$
$^{10}\text{C}$	19.3 s	1.9 MeV	$e^+$
$^{14}\text{O}$	71 s	5.15 MeV	$e^+$
$^{15}\text{O}$	122 s	2.76 MeV	$e^+$
$^{11}\text{C}$	20.38 min	0.96 MeV	$e^+$
$^{13}\text{N}$	9.97 min	2.22 MeV	$e^+$
$^7\text{Be}$	53 days	0.862 MeV	electron capture
$^{10}\text{Be}$	$1.5 \times 10^6$ years	0.556 MeV	$e^-$

Dominant production:  $^{12}\text{C}(\pi^-, ^3\text{He})$



# <sup>9</sup>Li Background

<sup>9</sup>Li events time window for prompt event:  
1sec after muon (<sup>9</sup>Li mean lifetime  
257msec)

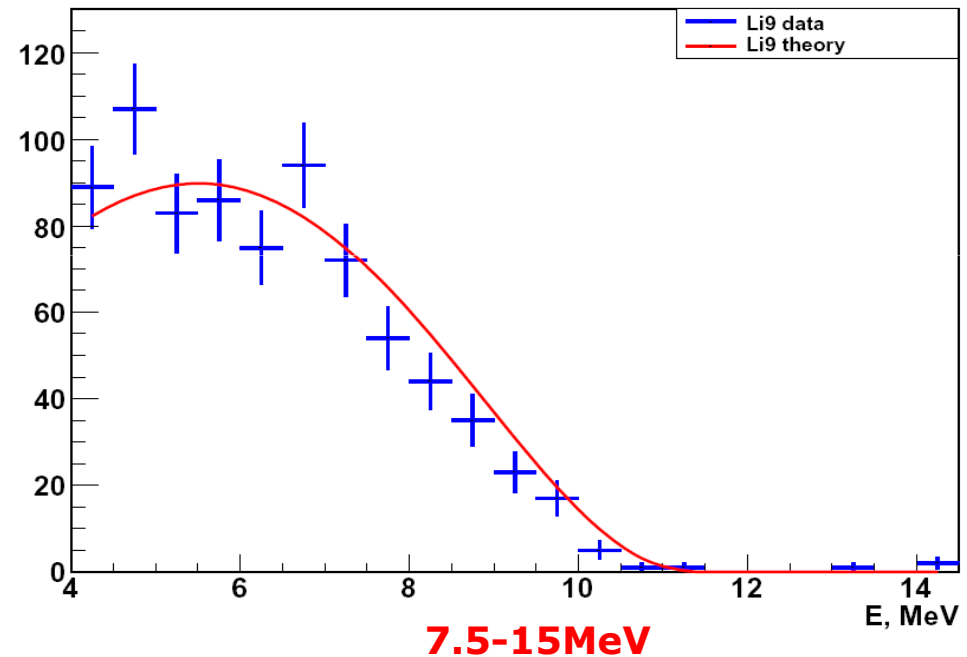
Background time window:  
5 to 6sec after muon

$R_{\text{prompt}}, R_{\text{delayed}} < 600\text{cm}$   
 $|R_{\text{prompt}} - R_{\text{delayed}}| < 160\text{cm}$   
 $dT < 1000\mu\text{sec}$   
 $E_{\text{prompt}}(\text{real}) > 4\text{MeV}$   
 $1.8\text{MeV} < E_{\text{delayed}}(\text{visible}) < 2.6\text{MeV}$

5.5m	4-15MeV		
	<sup>9</sup> Li events	BG	Li-BG
Showering muon	790	163	627
Non-showering muon	383	38	158

6.0m	4-15MeV		
	<sup>9</sup> Li events	BG	Li-BG
Showering muon	1026	216	810
Non-showering muon	498	293	205

$$\frac{N_{7.5-15\text{ MeV}}}{N_{4-15\text{ MeV}}} = 0.277$$



5.5m:  $173.7 \pm 8.6$ (showering muon) &  $43.7 \pm 6.6$ (non-showering muon)

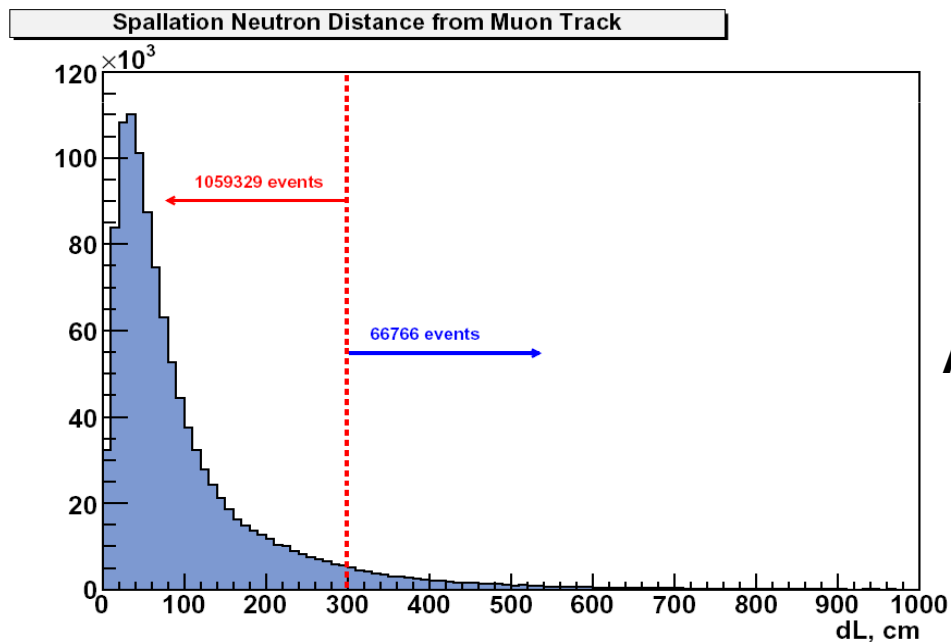
6.0m:  $224.4 \pm 9.7$ (showering muon) &  $56.8 \pm 7.8$ (non-showering muon)

Showering muon veto: 2sec veto for whole volume of the detector

Non-showering muon veto: 2sec veto around the muon track within 3m(delayed only)

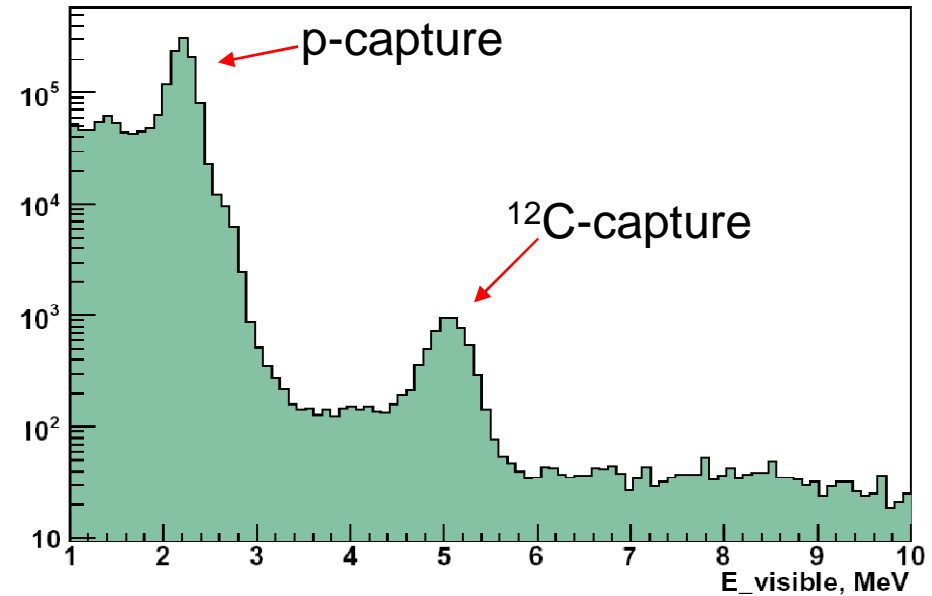
# $^9\text{Li}$ Background (spallation neutron)

Spallation neutron events time window:  
150-1000 $\mu\text{sec}$  after muon  
Off-timing background window:  
2150-3000 $\mu\text{sec}$  after muon



94.1% 3m cut efficiency

Spallation neutrons spectrum

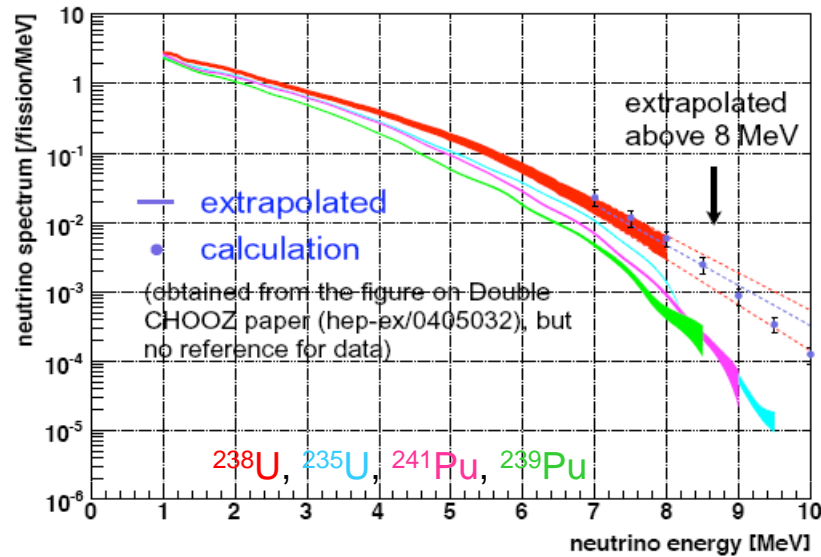


Applying 94.1% efficiency of 3m cut and 2sec cut total  $^9\text{Li}$  BG within 7.5-15MeV:

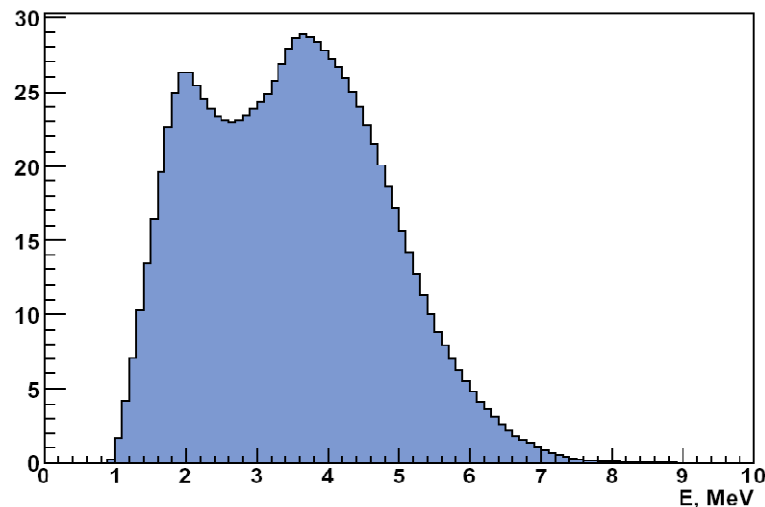
5.5m:  $2.7 \pm 0.4$  events

6.0m:  $3.5 \pm 0.5$  events

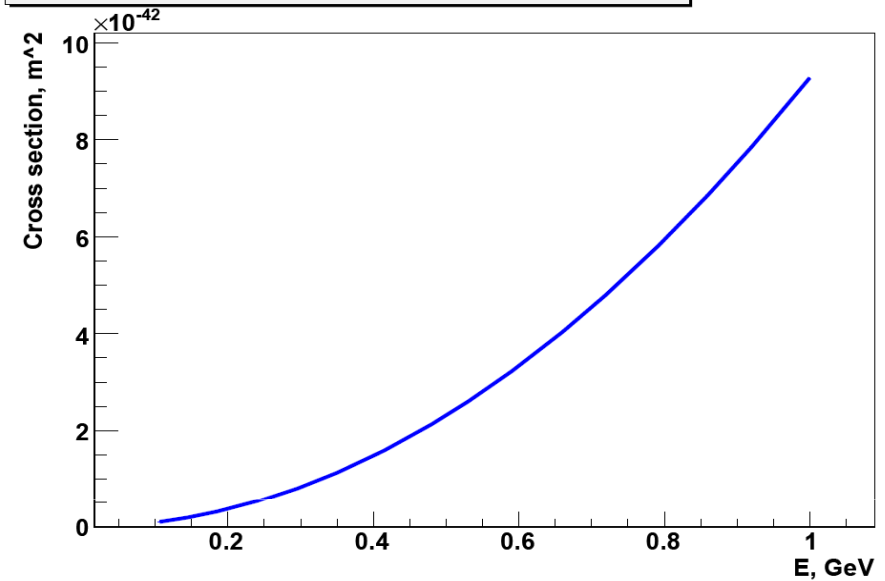
# Reactor neutrinos background



Prompt events energy spectrum



Cross section for electron antineutrino interaction on proton



KamLAND oscillation parameters:

$$\tan^2 \theta_{12} = 0.56$$

$$\Delta m_{21}^2 = 7.59 \times 10^{-5} \text{ eV}^2$$

**Background within 7.5-15 MeV:**

**5.5m:  $1.5 \pm 0.5$  events**

**6.0m:  $1.9 \pm 0.6$  events**

# Antineutrino background from atmospheric neutrinos interactions

## Neutral Current Interactions

$$\nu_{e,\mu} + {}^{12}\text{C} = n + {}^{11}\text{C} + \nu_{e,\mu}$$

$$\bar{\nu}_{e,\mu} + {}^{12}\text{C} = n + {}^{11}\text{C} + \bar{\nu}_{e,\mu}$$

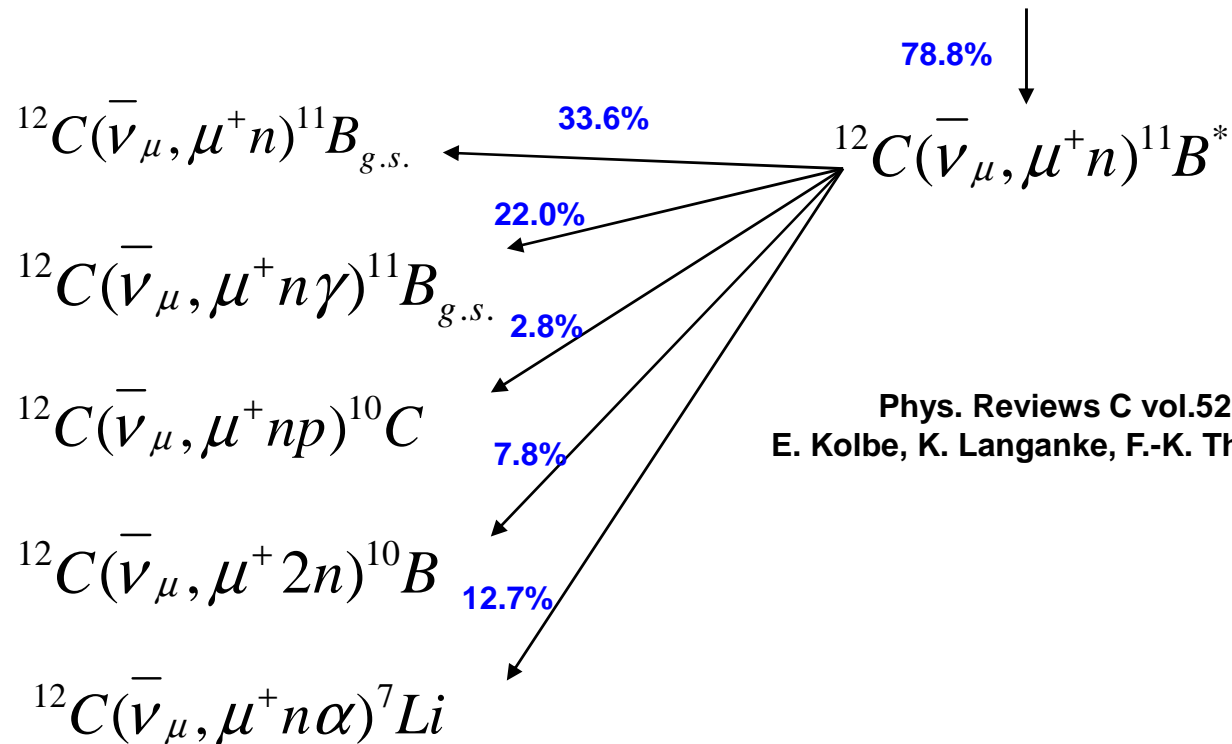
## Charged Current Interactions

$$1. \bar{\nu}_e + p = n + e^+$$

$$2. \bar{\nu}_\mu + p = n + \mu^+$$

$$3. \nu_\mu + {}^{12}\text{C} = \mu^- + n + {}^{11}\text{N}$$

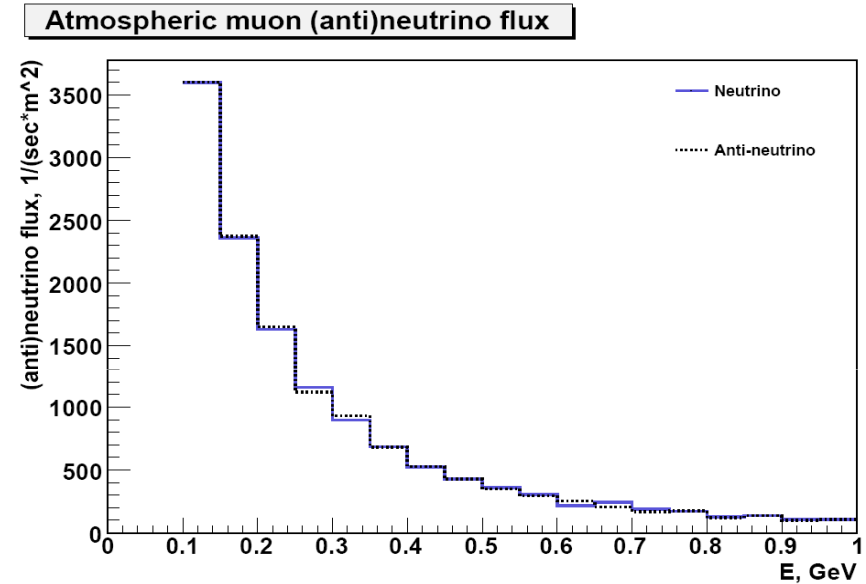
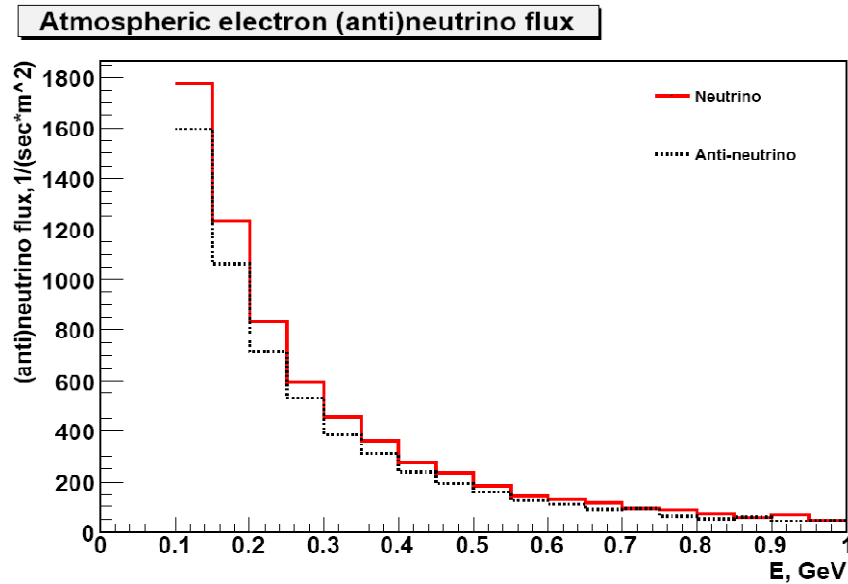
$$4. {}^{12}\text{C}(\bar{\nu}_\mu, \mu^+) X$$



Phys. Reviews C vol.52, number 6  
E. Kolbe, K. Langanke, F.-K. Thielmann, P. Vogel



# Atmospheric (anti)neutrino fluxes



Fluxes calculated by M. Honda for KamLAND detector position

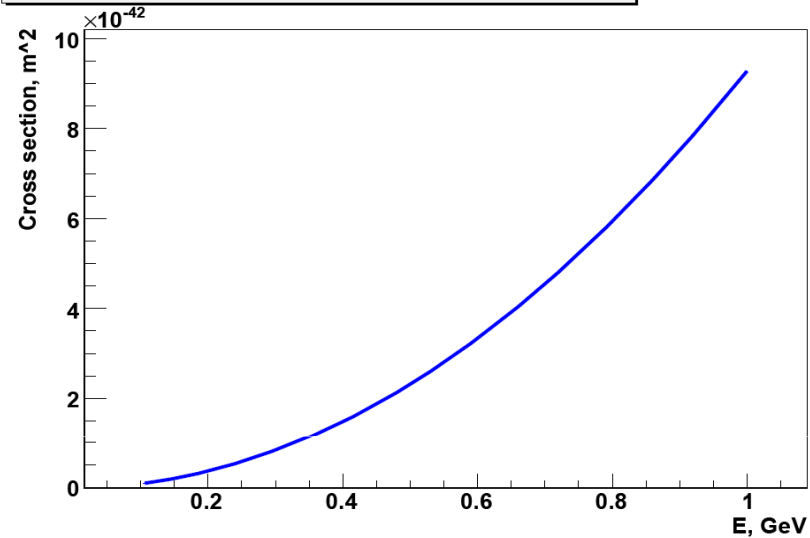
# MC simulation procedure for background calculation

- neutrino interactions distributed in LS+Buffer Oil
- tracking of secondary particles performed using GEANT package
- deposited energy quenched corresponding to results obtained by LS study with Compton Spectrometer at UT [ $K_B=0.01072 \text{ g}/(\text{MeV}\cdot\text{cm}^2)$ ] + contribution from Cherenkov light with reemission
- following cuts were applied:
  - $R < 6.0\text{m}$  for prompt and delayed events
  - $dR_{\text{prompt-delayed}} < 1.6\text{m}$
  - $dT_{\text{delayed-prompt}} < 1\text{msec}$
  - $1.8\text{MeV} < E_{\text{delayed}} < 2.6\text{MeV}$
  - $7.5\text{MeV} < E_{\text{prompt}} < 15\text{MeV}$

# Charged current interactions

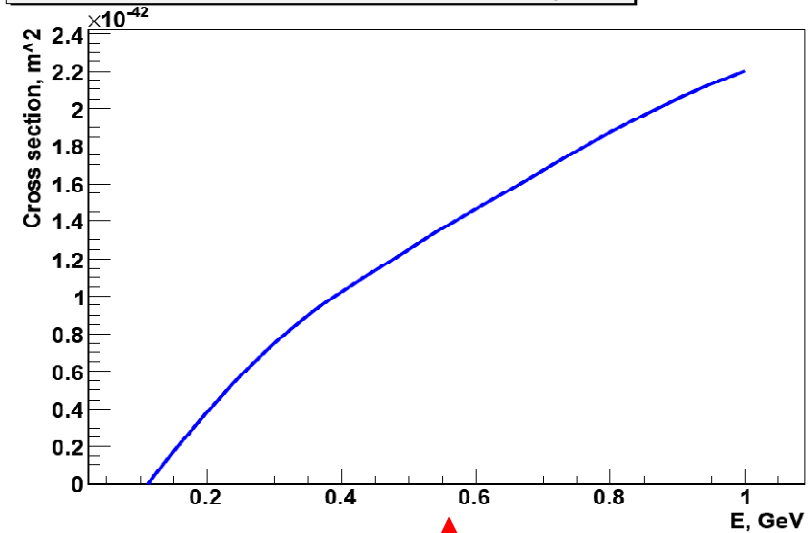
electron antineutrino interaction on proton

Cross section for electron antineutrino interaction on proton



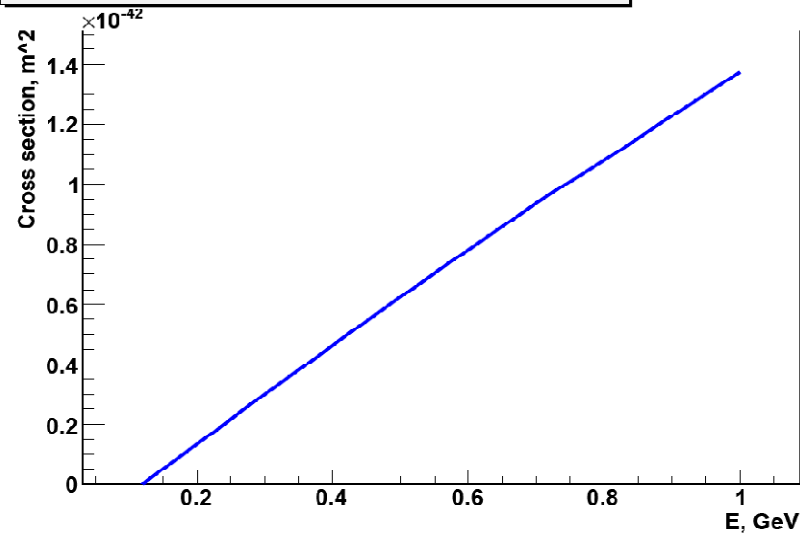
muon antineutrino interaction on proton

Cross section for muon antineutrino interaction on proton



muon antineutrino interaction on carbon

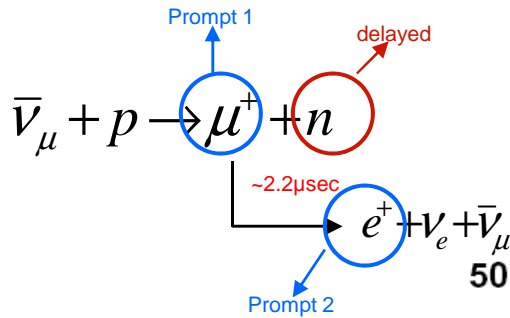
Cross section per nucleon for muon antineutrino interactions on carbon 12



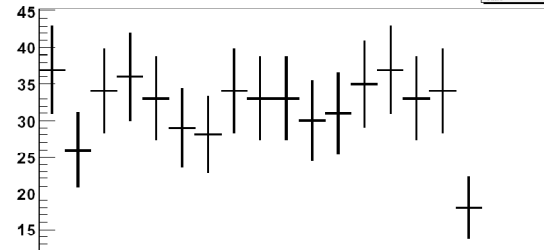
MiniBooNE calculations

M. Sajjad Athar, Shakeb Ahmad, S.K. Singh, Phys. Rev. D75:093003, 2007

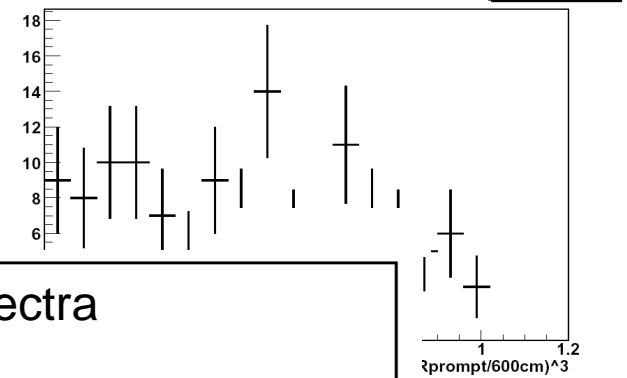
# CC interactions: Muon antineutrino on proton(6.0 m analysis)



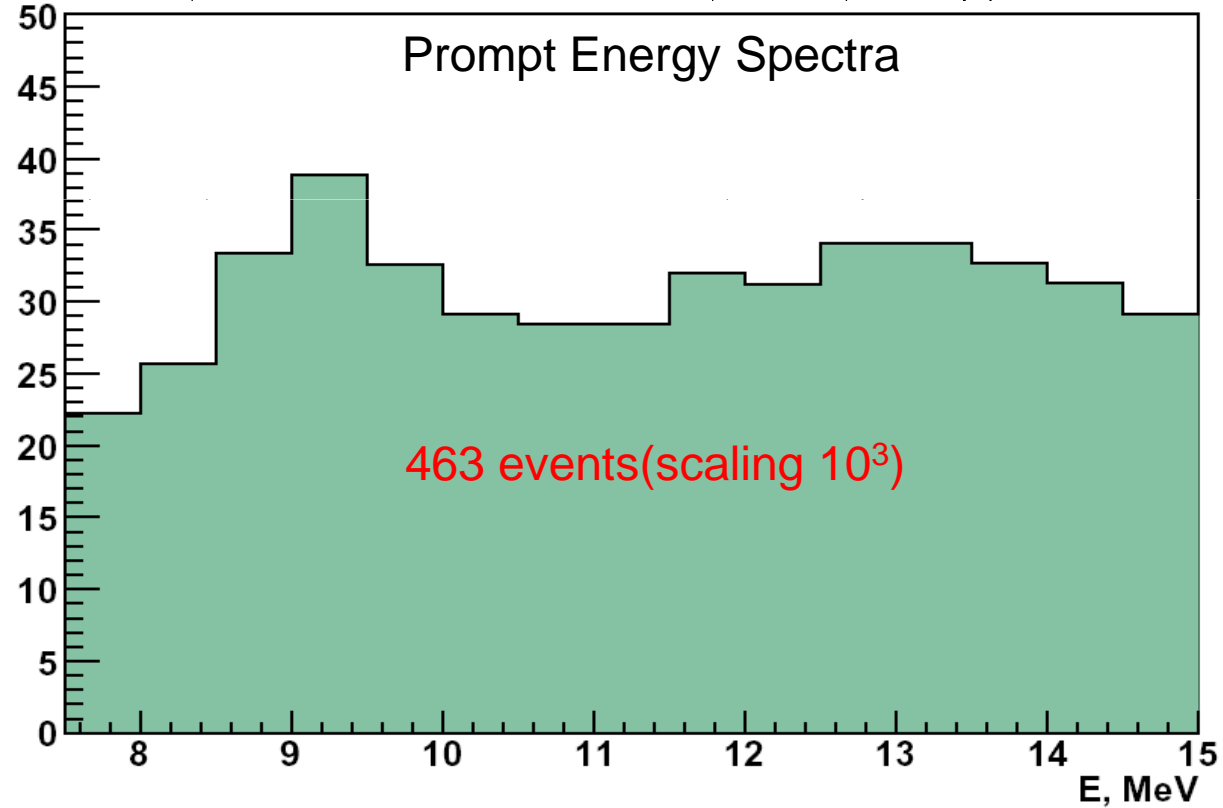
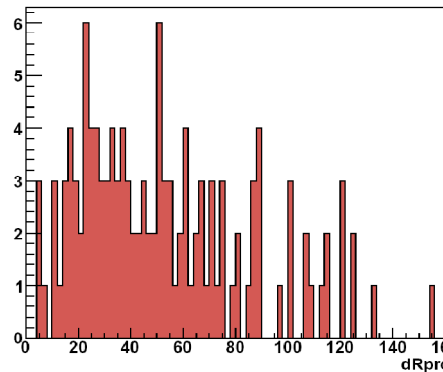
Muon Prompt spacial distribution 6m volume



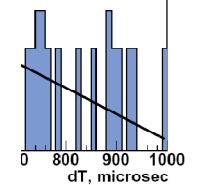
Positron prompt spacial distribution 6m volume



dR Positron prompt->delayed 6m volume



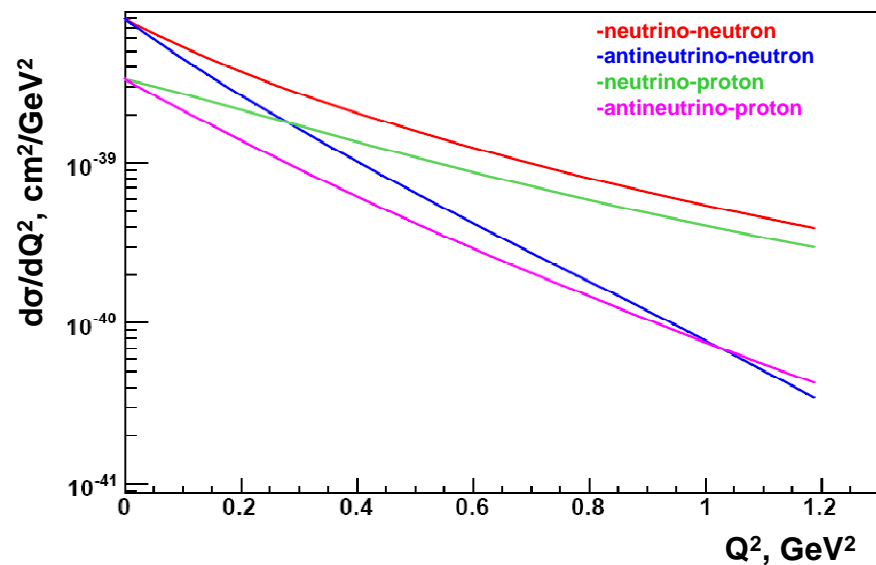
$\chi^2 / \text{ndf}$  77.77 / 80  
const  $22.06 \pm 1.86$   
t capture  $207.2 \pm 15.1$



# Neutral Current cross sections

$$\nu_{e,\mu} + {}^{12}\text{C} = n + {}^{11}\text{C} + \nu_{e,\mu}$$

Cross section of (anti)neutrino interactions  
on neutron and proton

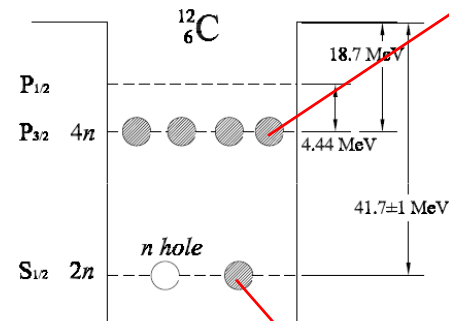


Neutrinos energy 1.25 GeV

$Q^2_{\text{max}} = 1.2 \text{ GeV}^2$

(L. A. Ahrens et al., Phys. Rev. D35, 785(1987))

+Nuclear Effects.

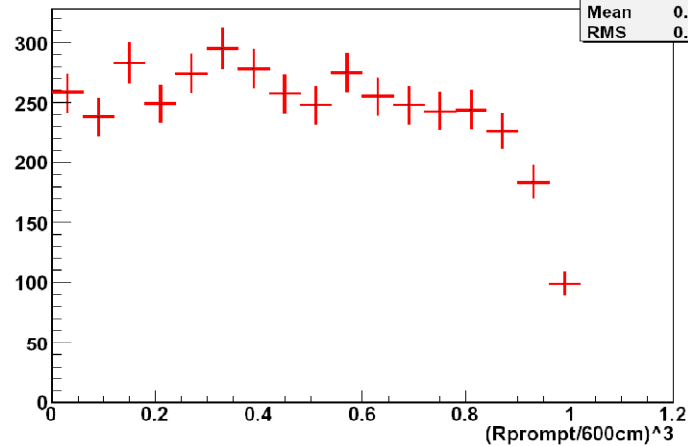


+Final States

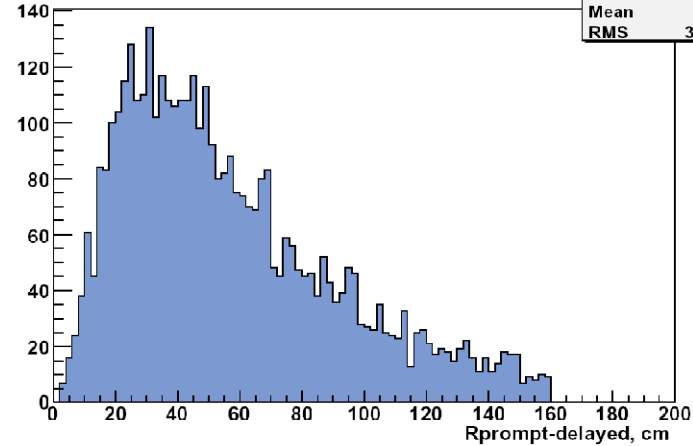
Decay mode	Daughter (decay, $T_{1/2}$ or $\Gamma$ , $Q_{EC}$ or $Q_{\beta^-}$ )	Mode %	Exp. sign. (hits)
${}^{11}\text{C}(\gamma)$	${}^{11}\text{C}_{gs}(\beta^+; 20.4 \text{ m}, 1.98 \text{ MeV})$	0.7	2
${}^{11}\text{C}(n, \dots)$	$\downarrow$	13.8	$\downarrow$
${}^{11}\text{C}(p, \dots)$	$\downarrow$	64.4	$\downarrow$
${}^{11}\text{C}(\alpha, \dots)$	$\downarrow$	21.1	$\downarrow$
${}^{11}\text{C}(n)$	${}^{10}\text{C}_{gs}(\beta^+; 19.3 \text{ s}, 3.65 \text{ MeV})$	3.0	3
${}^{11}\text{C}(n, \gamma)$	${}^{10}\text{C}_{gs}(\beta^+; 19.3 \text{ s}, 3.65 \text{ MeV})$	2.8	3
${}^{11}\text{C}(n, n)$	${}^9\text{C}(\beta^+; 0.127 \text{ s}, 16.5 \text{ MeV})$	0.06	4
${}^{11}\text{C}(n, p)$	${}^9\text{B}(p+2\alpha; 0.54 \text{ keV}, 1.07 \text{ MeV})$	5.7	2
${}^{11}\text{C}(n, \alpha)$	${}^6\text{Be}(2p+\alpha; 92 \text{ keV}, 4.3 \text{ MeV})$	2.2	2
${}^{11}\text{C}(p)$	${}^{10}\text{B}(\text{stable})$	2.9	1
${}^{11}\text{C}(p, \gamma)$	${}^{10}\text{B}(\text{stable})$	19.0	1
${}^{11}\text{C}(p, n)$	${}^9\text{B}(p+2\alpha; 0.54 \text{ keV}, 1.07 \text{ MeV})$	1.4	2
${}^{11}\text{C}(p, p)$	${}^9\text{Be}(\text{stable})$	7.2	1
${}^{11}\text{C}(p, \alpha)$	${}^6\text{Li}(\text{stable})$	33.9	1
${}^{11}\text{C}(\alpha)$	${}^7\text{Be}(\beta^+; 53.3 \text{ d}, 0.86 \text{ MeV})$	5.2	1*
${}^{11}\text{C}(\alpha, \gamma)$	${}^7\text{Be}(\beta^+; 53.3 \text{ d}, 0.86 \text{ MeV})$	4.2	1*
${}^{11}\text{C}(\alpha, n)$	${}^6\text{Be}(2p+\alpha; 92 \text{ keV}, 4.3 \text{ MeV})$	0.3	2
${}^{11}\text{C}(\alpha, p)$	${}^6\text{Li}(\text{stable})$	3.4	1
${}^{11}\text{C}(\alpha, \alpha)$	${}^3\text{H}(\beta^-; 12.3 \text{ y}, 18.6 \text{ keV})$	8.0	1*
${}^{11}\text{C}\{n, p\}$	${}^9\text{B}(p+2\alpha; 0.54 \text{ keV}, 1.07 \text{ MeV})$	7.1	2
${}^{11}\text{C}\{n, \alpha\}$	${}^6\text{Be}(2p+\alpha; 92 \text{ keV}, 4.3 \text{ MeV})$	2.5	2
${}^{11}\text{C}\{p, \alpha\}$	${}^6\text{Li}(\text{stable})$	37.3	1

# NC interactions: Outer shell (6.0 m analysys)

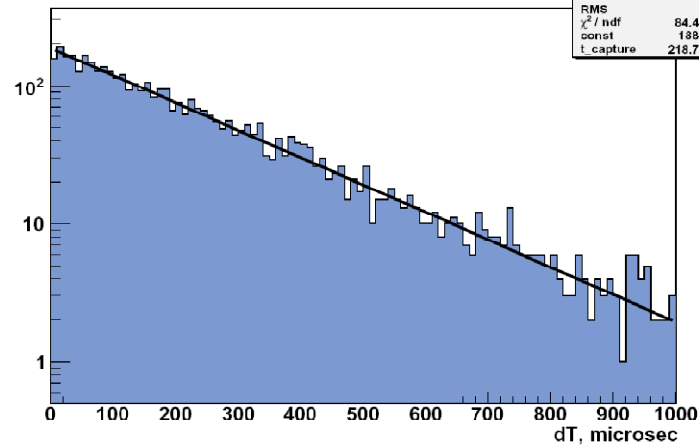
NC Prompt Spacial distribution 6m volume



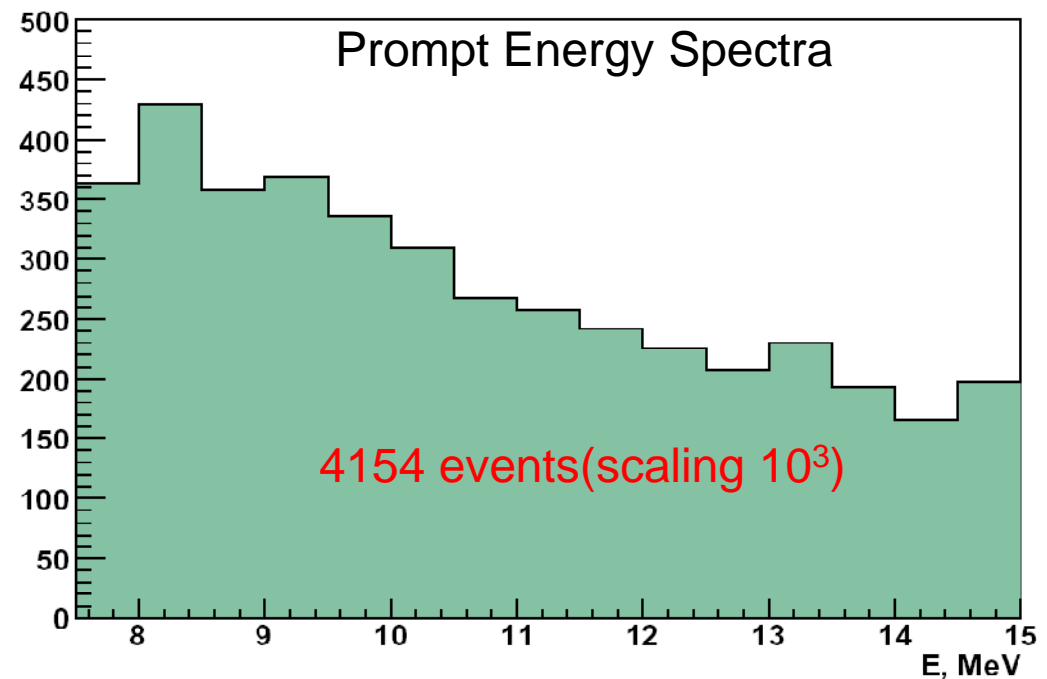
Distance Prompt->Delayed



NC Time difference prompt->delayed



Prompt Energy Spectra



# Background summary

## 5.5m analysis

	7.5-15MeV	Comments	15-30MeV	Comments
<b>Candidates</b>				
$\bar{\nu}_e + p \rightarrow e^+ + n$	6	1 multiple n-capture, 1 $\mu$ -decay	2	1 multiple n-capture, 1 $\mu$ -decay
<b>Charged Current Atmospheric Neutrinos Background</b>				
$\nu_\mu + {}^{12}\text{C} \rightarrow \mu^- + n + {}^{11}\text{N}$	0.046		0.154	
$\bar{\nu}_\mu + {}^{12}\text{C} \rightarrow \mu^+ + n + {}^{11}\text{B} + \gamma$	0.03		0.136	
$\bar{\nu}_\mu + {}^{12}\text{C} \rightarrow \mu^+ + n + {}^7\text{Li} + \alpha$	0.066		0.105	
$\bar{\nu}_\mu + {}^{12}\text{C} \rightarrow \mu^+ + 2n + {}^{10}\text{B}$	0.007		0.006	
$\bar{\nu}_\mu + {}^{12}\text{C} \rightarrow \mu^+ + n + {}^{11}\text{B}$	0.073		0.246	
$\bar{\nu}_\mu + p \rightarrow \mu^+ + n$	0.344		0.626	
$\bar{\nu}_e + p \rightarrow e^+ + n$	0.008		0.022	
<b>Neutral Current Atmospheric Neutrinos Background</b>				
$\nu + {}^{12}\text{C} \rightarrow \nu + n + {}^{11}\text{C}$	3.882		2.619	
Neutrino int. in the rock	0.1		0.05	
<b>Others</b>				
${}^9\text{Li}$	2.7		0	
Reactor anti neutrinos	1.5		0	
Accidental background	0.02		0	
<b>TOTAL Background</b>				
	8.776		3.964	

## 6.0m analysis

	7.5-15MeV	Comments	15-30MeV	Comments
<b>Candidates</b>				
$\bar{\nu}_e + p \rightarrow e^+ + n$	10	2 multiple n-capture, 1 $\mu$ -decay	6	2 multiple n-capture, 1 $\mu$ -decay
<b>Charged Current Atmospheric Neutrinos Background</b>				
$\nu_\mu + {}^{12}\text{C} \rightarrow \mu^- + n + {}^{11}\text{N}$	0.063		0.203	
$\bar{\nu}_\mu + {}^{12}\text{C} \rightarrow \mu^+ + n + {}^{11}\text{B} + \gamma$	0.048		0.185	
$\bar{\nu}_\mu + {}^{12}\text{C} \rightarrow \mu^+ + n + {}^7\text{Li} + \alpha$	0.087		0.136	
$\bar{\nu}_\mu + {}^{12}\text{C} \rightarrow \mu^+ + 2n + {}^{10}\text{B}$	0.005		0.009	
$\bar{\nu}_\mu + {}^{12}\text{C} \rightarrow \mu^+ + n + {}^{11}\text{B}$	0.1		0.324	
$\bar{\nu}_\mu + p \rightarrow \mu^+ + n$	0.463		0.837	
$\bar{\nu}_e + p \rightarrow e^+ + n$	0.011		0.028	
<b>Neutral Current Atmospheric Neutrinos Background</b>				
$\nu + {}^{12}\text{C} \rightarrow \nu + n + {}^{11}\text{C}$	5.144		3.449	
Neutrino int. in the rock	0.13		0.07	
<b>Others</b>				
${}^9\text{Li}$	3.5		0	
Reactor anti neutrinos	1.9		0	
Accidental background	0.163		0.001	
<b>TOTAL Background</b>				
	11.614		5.242	

- NC cross-section uncertainty 18%
- Atmospheric neutrino flux uncertainty 22%
- Combined uncertainty 28.4%

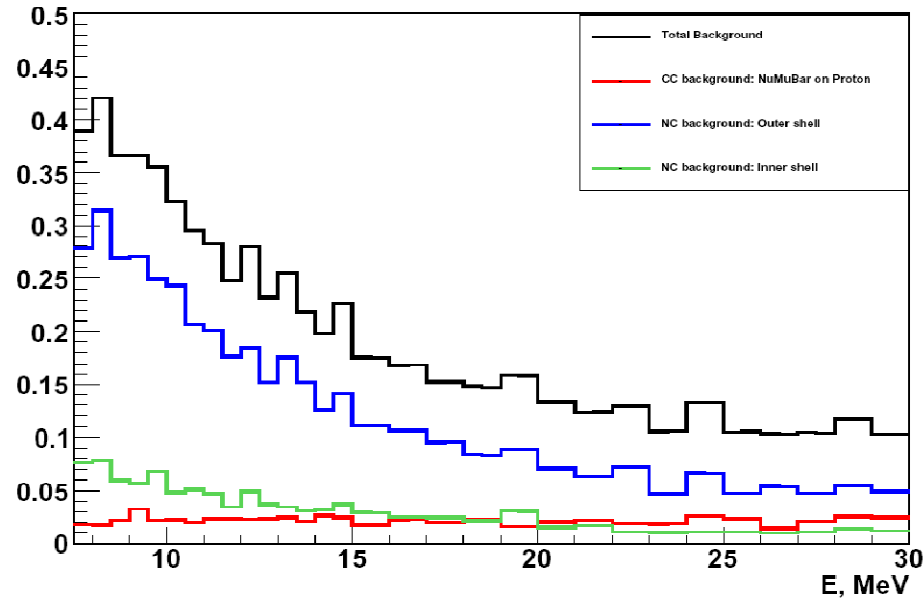
**Total BG within 7.5-15MeV:**  
**5.5m:  $8.78 \pm 2.16$  events**  
**6.0m:  $11.61 \pm 2.78$  events**

**Total BG within 15-30MeV:**  
**5.5m:  $3.96 \pm 1.04$  events**  
**6.0m:  $5.24 \pm 1.38$  events**

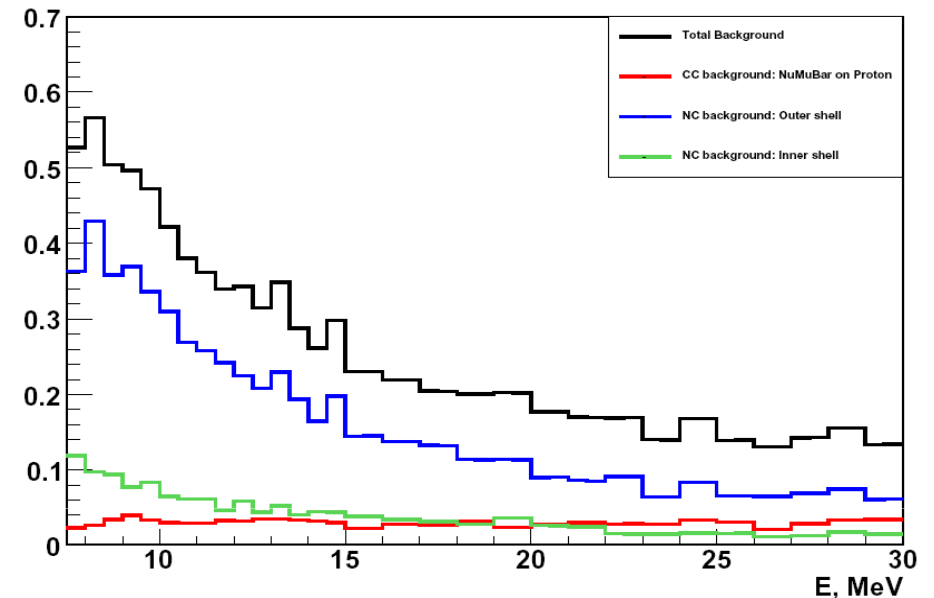


# Atmospheric background in 7.5-30 MeV

Atmospheric neutrinos background 5.5m volume



Atmospheric neutrinos background 6m volume



## Triple coincidence summary

7.5-15MeV							
DATA				Background			
5.5m volume		6.0m volume		5.5m volume		6.0m volume	
multi n-capture	$\mu$ -decay	multi n-capture	$\mu$ -decay	multi n-capture	$\mu$ -decay	multi n-capture	$\mu$ -decay
1	1	2	1	0.05	0.02	0.07	0.09

# New Limits on Solar Antineutrino Flux

$$\Phi_{\bar{\nu}_e} = \frac{N_{\text{signal}}}{\sigma \times \varepsilon \times T \times n_{\text{protons}}}$$

- $N_{\text{signal}}$  – mean signal obtained with 95% C.L. for known number of the selected candidates and B.G.
- $\sigma = 6.9 \times 10^{-42} \text{cm}^2$  averaged cross-section
- $\varepsilon = 0.94$  detection efficiency
- $T = 1.2 \times 10^8 \text{sec}$  livetime
- $n_{\text{protons}} = 4.6 \times 10^{31} (5.5\text{m})$  and  $6.0 \times 10^{31} (6.0\text{m})$

Upper limits on solar electron antineutrino flux for 8.8-16.3MeV:

$$\Phi_{\bar{\nu}_e} < 1.2 \times 10^2 \text{ cm}^{-2} \text{ s}^{-1} \text{ for } 5.5\text{m}$$

$$\Phi_{\bar{\nu}_e} < 1.3 \times 10^2 \text{ cm}^{-2} \text{ s}^{-1} \text{ for } 6.0\text{m}$$

Current best limit was improved by factor of 3.6 normalizing to the energy range

8.8-16.3MeV energy range contains 24.05% of the total  $^8\text{B}$  neutrino flux  $5.05 \times 10^6 \text{cm}^{-2} \text{s}^{-1}$

**Neutrino conversion probability:**  
 **$P < 9.8 \times 10^{-5} (5.5\text{m volume})$**

product of neutrino magnetic moment and magnetic field in the core of the Sun:

$$\frac{\mu}{10^{-12} \mu_B} \frac{B_T (0.05 R_s)}{10 \text{kG}} < 7.7 \times 10^2$$

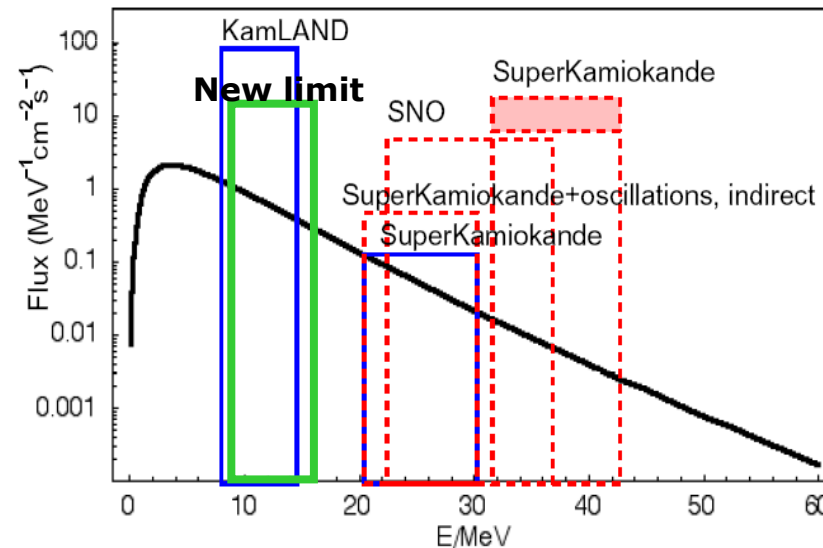
# Limit on the diffuse Supernovae neutrino flux

Core-collapse Supernovae rate in the Universe is  $\sim 1$  per second with neutrino emission rate  $\sim 10^{58}$  in one collapse

Current and future neutrino detectors have a possibility to detect cumulative neutrino flux from all past Core-collapse Supernovae

## Current limits on DSNF

From: C.Lunardini, astro-ph/0610534

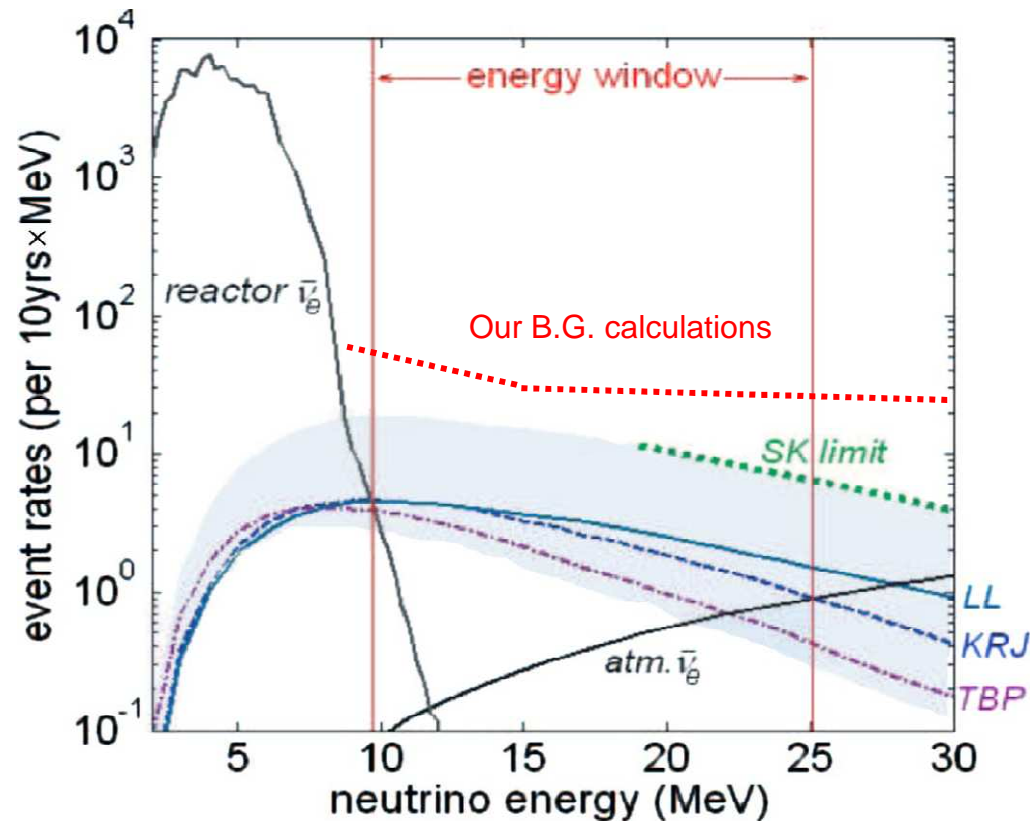


Observed limit on the electron antineutrinos from the Sun can be used for DSNF

New limit is  $16 \text{ cm}^{-2} \text{ s}^{-1} \text{ MeV}^{-1}$

# Future neutrino detectors

Event rates in future LENA, 50 kt liquid scintillator detector from the various neutrino sources (LENA proposal Phys.Rev.D75:023007)



B.G. rate from NC interactions of the atmospheric neutrinos is significantly higher than expected DSNF

# Conclusion

## •Methodology:

Based on the Compton Spectrometer measurements with KamLAND liquid scintillator we found Birks' Coefficient for electrons:

$$K_B = 0.01072 \text{ g} \cdot \text{MeV}^{-1} \cdot \text{cm}^{-2}$$

•Physics: We obtained new limit on electron antineutrino flux from the Sun within 8.8-16.3 MeV neutrino energy range at 95% C.L.:

$$\Phi_{\bar{\nu}_e} < 1.2 \times 10^2 \text{ cm}^{-2} \text{ s}^{-1}$$

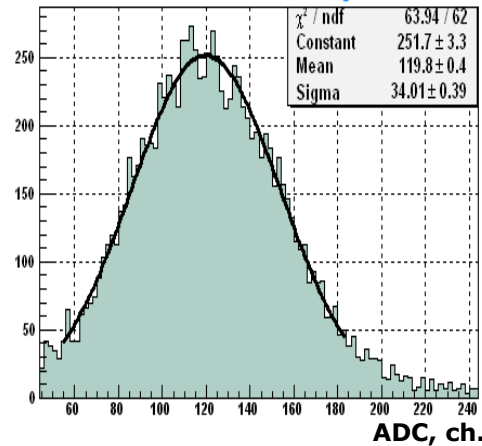
This limit corresponds to an upper limit on the neutrino conversion probability of  $9.8 \times 10^{-5}$  at 95% C.L. Observed limits improved by factor of 3.6 with respect to previous KamLAND result. More statistics will not significantly improve these limits. Same limit can be used for Diffuse Supernovae Neutrino Flux

Calculations of background induced by neutral current interactions of atmospheric neutrinos in scintillator are important for the development of future large scintillator neutrino detectors

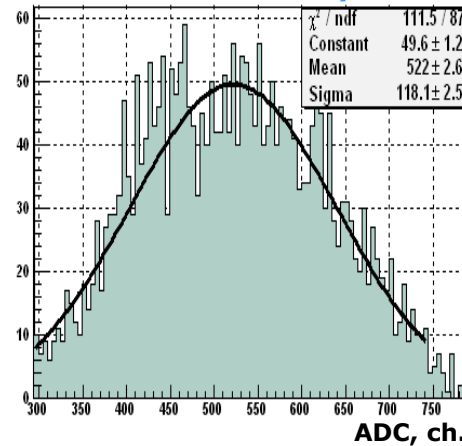
Backup slides

# Tyvek VS. no Tyvek

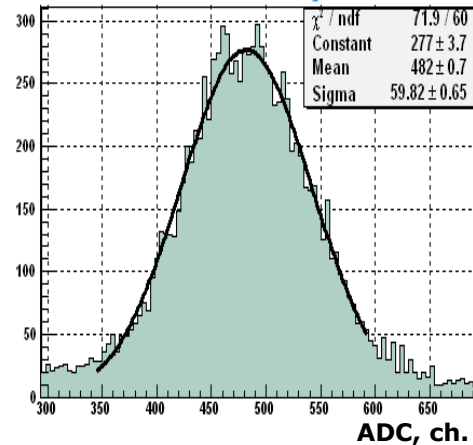
0.511MeV no Tyvek



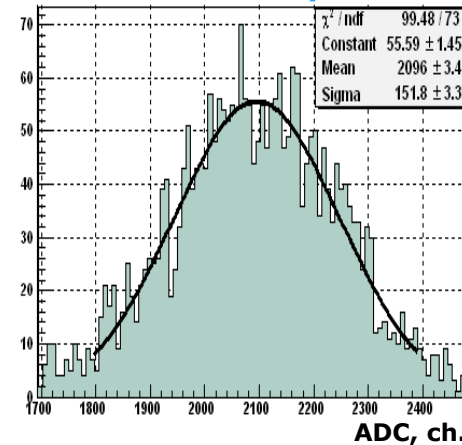
1.275MeV no Tyvek



0.511MeV Tyvek



1.275MeV Tyvek



	No Tyvek		Tyvek	
Incident gamma E, MeV	0.511	1.275	0.511	1.275
Mean, ch.	119.8	522	482	2096
Sigma, ch.	34.01	118.1	59.82	151.8
Resolution, %	28.4 $\pm 0.3$	22.6 $\pm 0.5$	12.4 $\pm 0.1$	7.2 $\pm 0.2$

Light collection gain with Tyvek is 4.02

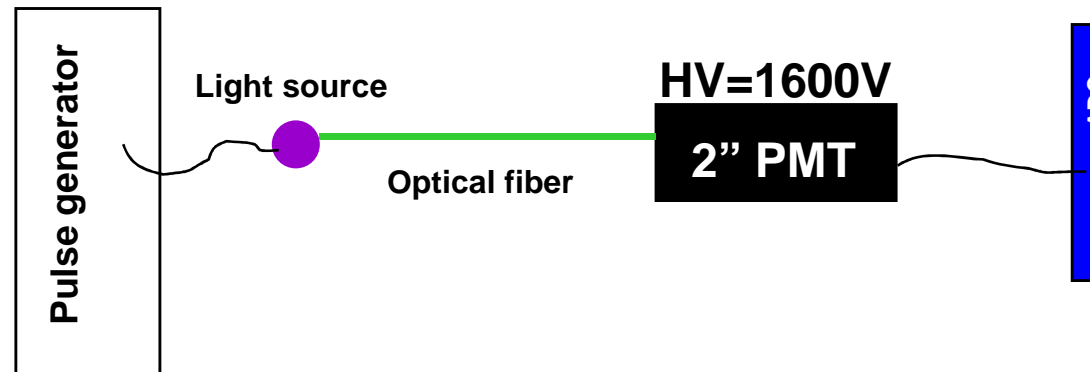
Tyvek did not change the ratio between deposited energies for both peaks  $E_1/E_2=4.35$

This result shows the linearity of the PMT

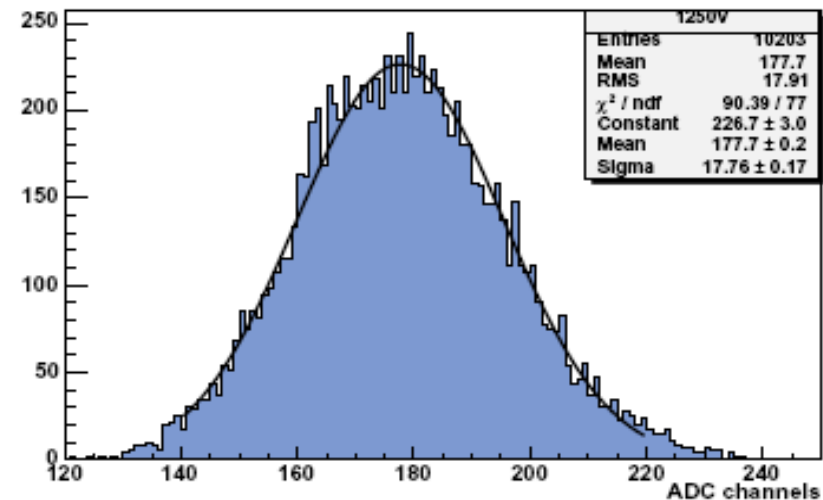
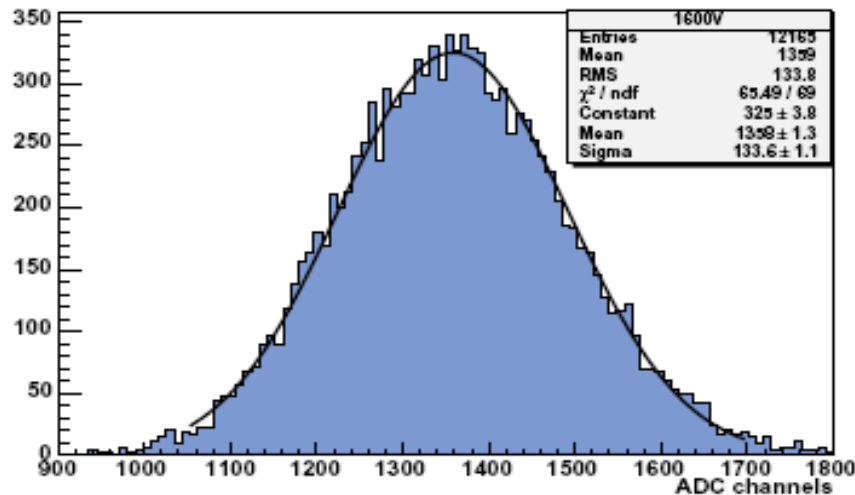
Measurements were made at 60 degrees



# Scintillator light output calibration

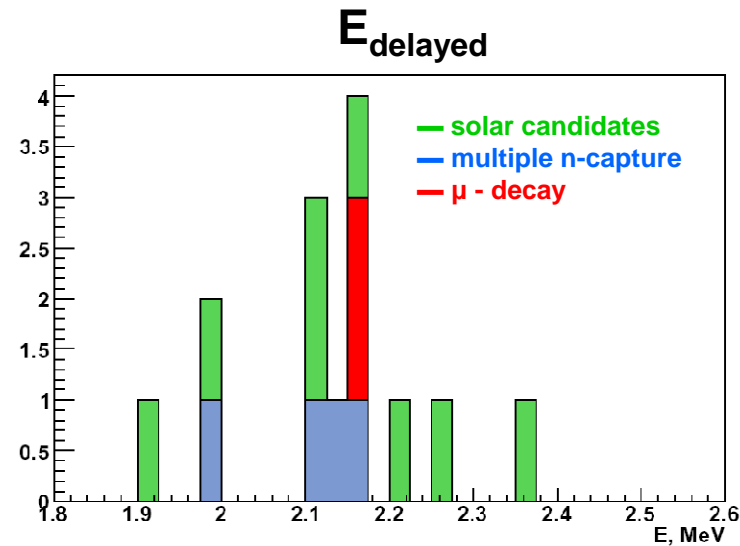
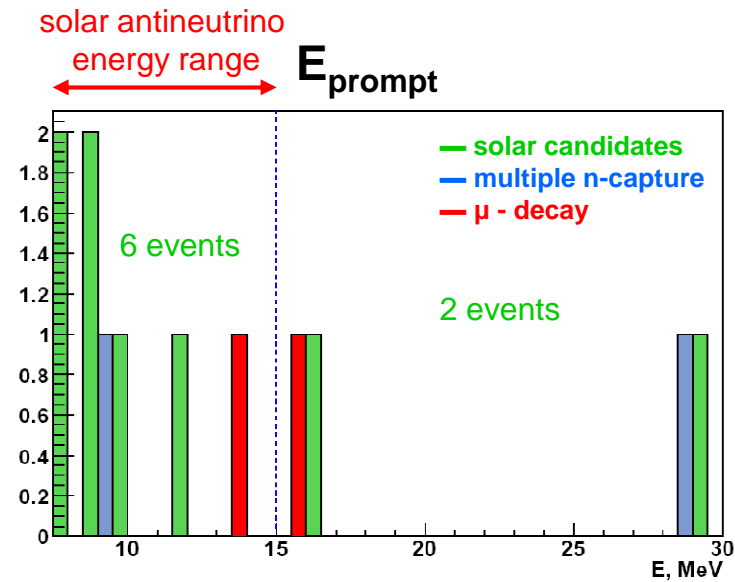


Single photoelectron have been seen with HV=1600V



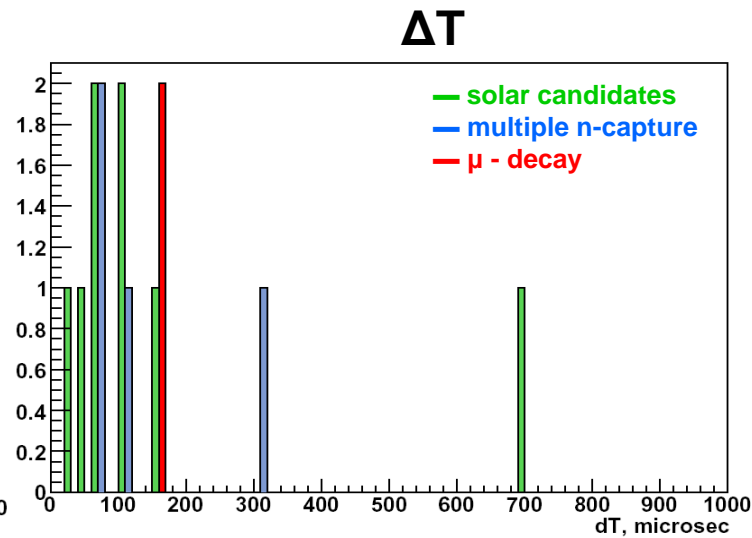
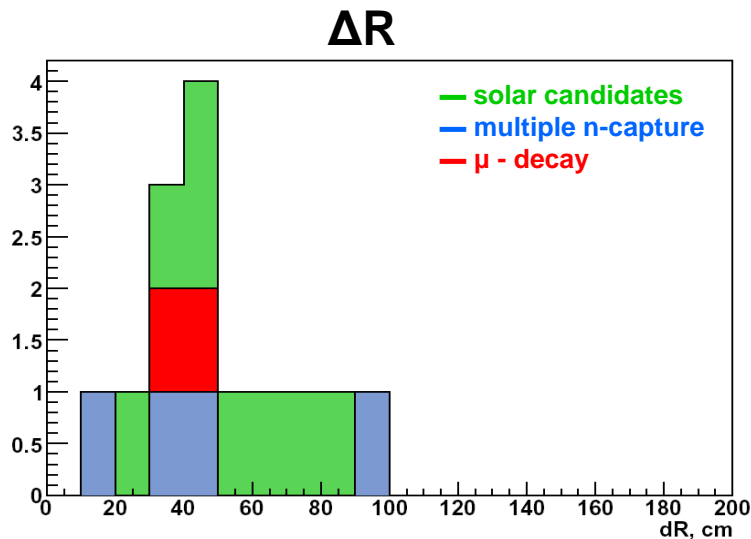
PMT gain between 1250V and 1600V is 7.65

# High Energy Candidates 5.5m fiducial volume



7.5-15 MeV:  
6 candidates has been selected  
+  
1 triple coincidence:  
multiple neutrons capture  
Run# 1824, Prompt# 13658585  
Delayed# 13658586, 13658587

+



1 muon decay  
(triple coincidence)  
Run# 5380  
Prompt\_1# 41470(muon, E=15.5 MeV)  
Prompt\_2# 41471(positron, E=13.6 MeV)  
Delayed# 41472  
 $dT_{1-2} = 1.23 \mu\text{sec}$   
 $dR_{1-2} = 6.4 \text{ cm}$